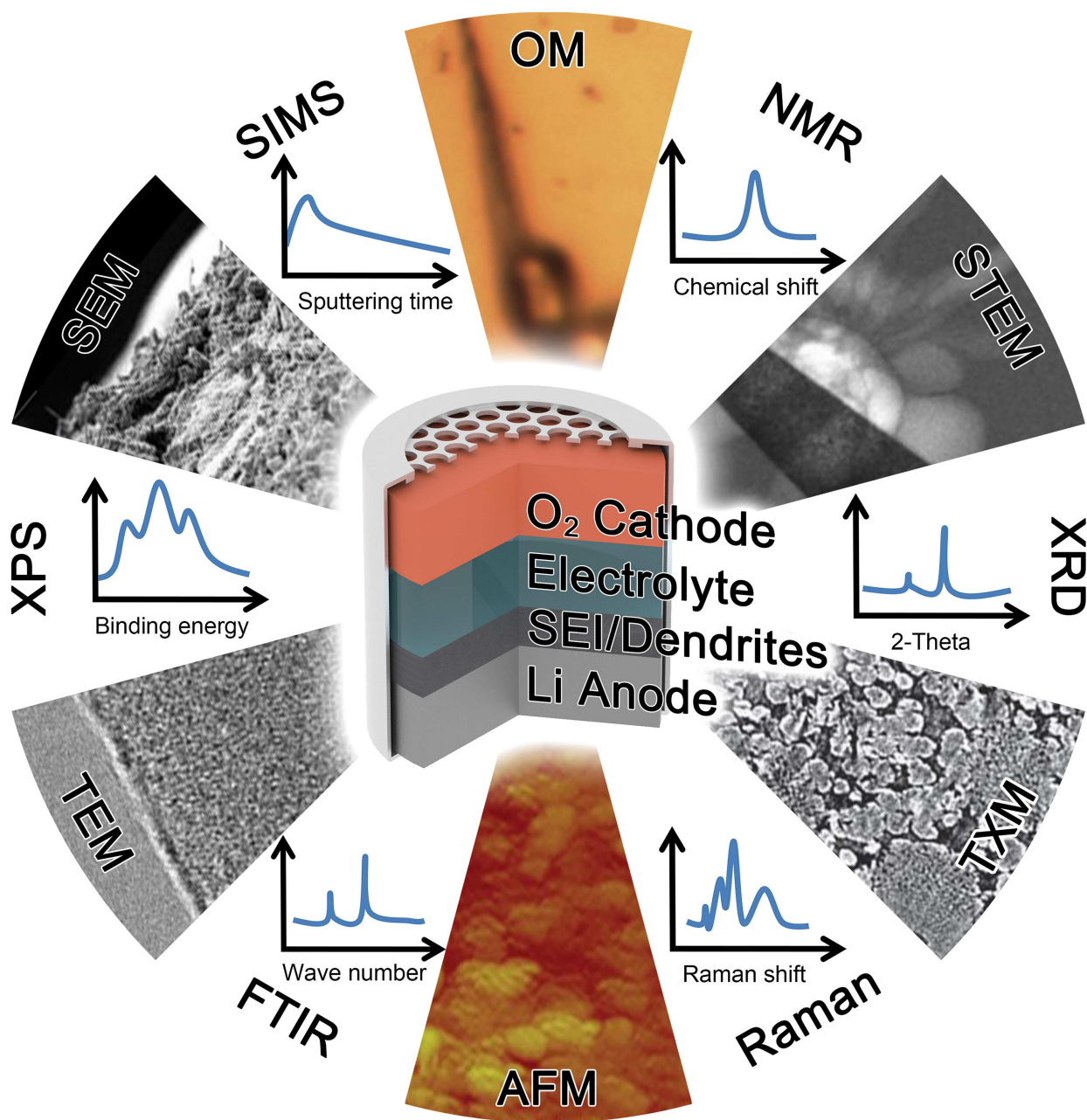


# Safe Lithium-Metal Anodes for Li–O<sub>2</sub> Batteries: From Fundamental Chemistry to Advanced Characterization and Effective Protection

Yan-Shuai Hong<sup>+, [a, b]</sup> Chen-Zi Zhao<sup>+, [c]</sup> Ye Xiao<sup>+, [d, e]</sup> Rui Xu,<sup>[d, e]</sup> Jing-Jing Xu,<sup>[a]</sup> Jia-Qi Huang,\*  
<sup>[d, e]</sup> Qiang Zhang,\*<sup>[c]</sup> Xiqian Yu,\*<sup>[a, b]</sup> and Hong Li<sup>[a, b]</sup>



Rechargeable Li–O<sub>2</sub> batteries play an increasing important role as energy storage devices, which have both, a high capacity anode and a cathode using an inexhaustible resource. As a key component in Li–O<sub>2</sub> batteries, the Li-metal anode suffers from major drawbacks related to Li dendrite formation and SEI layer growth, which are also major issues for Li-metal rechargeable batteries. This review presents an overview on the scientific challenges, fundamental mechanisms and modification strategies of Li-metal anodes for Li–O<sub>2</sub> batteries. Firstly, basic principles and challenges on Li-metal anodes are briefly retrospected. We further summarize and categorize the prevailing characterization techniques based on Li dendrite morphology characterization and SEI composition analysis. The up-to-

date development of in-situ and operando characterization is also included. Following the obtained insights, effective protection/modification strategies towards practical application for Li–O<sub>2</sub> batteries are presented. Furthermore, we highlight the significance of advanced characterization techniques in interrogating the buried keys for solving practical hindrances for Li–O<sub>2</sub> batteries. The comprehensive characterization and analysis of Li anodes, cathodes, and electrolytes by various methods together with the development of novel techniques are expected to be indispensable to gain a thorough understanding of the battery operation and for offering guidelines for their practical development.

## 1. Introduction

Society is calling for the energy storage that can meet the demands of unpredictable and everlasting energy supply and generation nowadays. Batteries have aroused increasing interests in the development of electric vehicles, portable electronics and renewable sources, accelerating their wide propagations to nearly every corner of our lives.

In the past decades, myriad technologies for rechargeable batteries have been explored, such as Lead-acid, Nickel-cadmium (Ni–Cd), Nickel-metal hydride (Ni–MH) and Li-ion batteries.<sup>[1]</sup> Among those available options, rocking-chair Li-ion secondary batteries usually containing a transition-metal oxide cathode and a graphite anode have been investigated with significant efforts and achieved a spectacular success since their introduction in early 1990s.

However, a strong motivation for developing alternatives beyond Li-ion batteries exists presently as the current Li-ion battery technology is reaching its upper limit. New chemistry

and materials are actively sought with formidable challenges to achieve the higher energy density and low cost.

## 2. Li–O<sub>2</sub> Battery Chemistry

To move a leap forward, migrating from Li-ion to lithium-air battery is one of the most promising solutions for next generation energy storage devices. The rechargeable Li–O<sub>2</sub> batteries yield extremely high theoretical specific energy and energy density by employing the air-breathing cathode and Li-metal anode. In the fully discharged state, they reach the energy density of 3458 Wh kg<sup>-1</sup> and 3445 Wh L<sup>-1</sup> based on the product Li<sub>2</sub>O<sub>2</sub>, which is one of the highest theoretical values among various secondary batteries.<sup>[2]</sup> Besides, the cost of Li–O<sub>2</sub> batteries may be lowered compared to Li-ion batteries with transition-metal oxides due to the active material oxygen in cathode is available in atmosphere.<sup>[3]</sup>

The most conventional configuration of Li–O<sub>2</sub> batteries consists of a porous cathode to collect oxygen and accommodate oxygen electrochemical reactions, a metallic Li anode as lithium source to store charge, and an electrolyte system for Li ions conduction. In most cases, O<sub>2</sub> derived from the air accesses the cathode, dissolves in the electrolyte, meets Li ions and is reduced during discharge.<sup>[4]</sup> On the anode side, metallic Li is oxidized on discharge and recovered on charge.

Moving from theory to practice, four architectures can be classified according to the type of electrolyte: aqueous, non-aqueous, hybrid, and solid-state system.<sup>[5]</sup> It is emphasized that all these systems have employed Li-metal anode, instead of graphite anode in traditional Li-ion battery, for higher energy gains to realize the competitive energy density of Li–O<sub>2</sub> chemistry.<sup>[6]</sup>

In aqueous Li–O<sub>2</sub> batteries, oxygen and water react with Li to form LiOH·H<sub>2</sub>O in an alkaline electrolyte and this reaction is reversed during charge process. Although there are some research activities on the aqueous Li–O<sub>2</sub> battery, the accelerated deterioration of Li metal electrode in aqueous environment, pH changes during cycling, low decomposition voltage and much limited theoretical specific energy have hindered its application.

- [a] Y.-S. Hong,<sup>†</sup> Dr. J.-J. Xu, Prof. X. Yu, Prof. H. Li  
Beijing Advanced Innovation Center for Materials Genome Engineering,  
Institute of Physics, Chinese Academy of Sciences  
Beijing 100190, China  
E-mail: xyu@iphy.ac.cn
- [b] Y.-S. Hong,<sup>†</sup> Prof. X. Yu, Prof. H. Li  
Center of Materials Science and Optoelectronics Engineering  
University of Chinese Academy of Sciences  
Beijing 100049, China
- [c] C.-Z. Zhao,<sup>†</sup> Prof. Q. Zhang  
Beijing Key Laboratory of Green Chemical Reaction Engineering and Technology, Department of Chemical Engineering  
Tsinghua University  
Beijing 100084, China  
E-mail: zhang-qiang@mails.tsinghua.edu.cn
- [d] Y. Xiao,<sup>†</sup> R. Xu, Prof. J.-Q. Huang  
School of Materials Science and Engineering  
Beijing Institute of Technology  
Beijing 100081, China  
E-mail: jqhuang@bit.edu.cn
- [e] Y. Xiao,<sup>†</sup> R. Xu, Prof. J.-Q. Huang  
Advanced Research Institute of Multidisciplinary Science  
Beijing Institute of Technology  
Beijing 100081, China
- [†] These authors contributed equally to this work.

For non-aqueous Li–O<sub>2</sub> batteries, oxygen gas is captured and widely regarded to be catalytically reduced to solid Li<sub>2</sub>O<sub>2</sub>: 2Li<sup>+</sup><sub>(l)</sub> + O<sub>2</sub><sub>(g)</sub> + 2e<sup>-</sup> = Li<sub>2</sub>O<sub>2</sub><sub>(s)</sub> (2.96 V vs Li/Li<sup>+</sup>), delivering a high gravimetric and volumetric energy density.<sup>[7]</sup> This process involves a complicated reaction with multiple steps, where superoxide radical intermediates of high deprotonation activity are produced, thus the Li-metal anode suffers from the corrosion from the crossover of air, the cathode reaction products and electrolyte decompositions. In the past few decades, a majority of efforts have been dedicated to the non-aqueous batteries since Abraham first reported a Li–O<sub>2</sub> battery

containing porous cathode, organic electrolyte and metallic Li anode. Presently non-aqueous Li–O<sub>2</sub> batteries are regarded to exhibit higher probability of commercialization compared with their aqueous counterpart.

Hybrid Li–O<sub>2</sub> systems achieve a reduction of oxygen in an alkaline electrolyte and metallic Li dissolution in a non-aqueous electrolyte in one battery, where an ionic conductor separator with high stability on both sides is of vital importance.<sup>[8]</sup>

Solid-state batteries are expected to solve the safety issues and enhance the energy density by protecting Li anode from the crossover of oxygen and moisture in air and electrolyte



Yan-Shuai Hong received his B. Eng from School of Physical Science and Technology in Lanzhou University (2017). He is now a Ph.D. candidate in Institute of Physics, Chinese Academy of Sciences. His main areas of research address energy-storage materials, including cathode materials for lithium-ion and solid state lithium batteries.



Chen-Zi Zhao obtained her B. Eng from School of Materials Science and Engineering in Tsinghua University (2015). She is now a Ph.D. candidate in Department of Chemical Engineering, Tsinghua University. Her main areas of research address energy-storage materials, including electrolytes and lithium metal anodes.



Ye Xiao received his B.Eng. (2018) degree in Chemical Engineering from Beijing Institute of Technology, China. He is currently a master student under the supervision of Prof. Jia-Qi Huang at Advanced Research Institute of Multidisciplinary Science (ARIMS), Beijing Institute of Technology. His research interests focus on the interface chemistry for stable lithium metal anodes towards high energy density batteries.



Rui Xu received his B.Eng. (2017) degree in Chemical Engineering from Beijing Institute of Technology, China. He is currently a Ph.D. student under the supervision of Prof. Jia-Qi Huang at Advanced Research Institute of Multidisciplinary Science (ARIMS), Beijing Institute of Technology. His research interests focus on the interface chemistry investigation and rational design for lithium metal anodes interfaces.



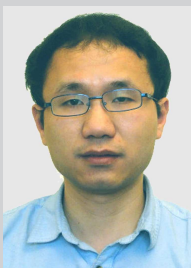
Jingjing Xu received her B.S (2011) degree from Northwest A&F University and her Ph.D (2018) degree from Xi'an Jiaotong University. Now she is a postdoc under the supervision of Prof. Hong Li at Institute of Physics, Chinese Academy of Sciences. Her research interests concern solid-state batteries, including solid-state electrolytes and composite lithium metal anodes.



Jia-Qi Huang received his B.Eng. (2007) and Ph.D. (2012) degree in Chemical Engineering from Tsinghua University, China. He is currently a professor at Advanced Research Institute of Multidisciplinary Science (ARIMS), Beijing Institute of Technology. His research interests focus on the chemistry in advanced energy storage/conversion materials, including Li-S batteries, Li-metal anodes, etc.



Qiang Zhang received his bachelor and Ph.D. degree from Tsinghua University, China in 2004 and 2009, respectively. Now he is a full professor at Tsinghua University. His current research interests are advanced energy materials, including lithium sulfur batteries, lithium metal anode, and electrocatalysis.



Xiqian Yu is currently a professor at Institute of Physics, Chinese Academy of Sciences (IOP, CAS). He received this Bachelor's degree (2005) from Wuhan University and PhD degree in condensed matter physics (2010) from IOP, CAS. Prior to IOP, he worked at Brookhaven National Laboratory as a postdoctoral fellow (2010-2013) and Physics Associate (2013-2016). His research interest is in the field of electrochemical energy storage with the main focus on the characterization of the electrode materials for rechargeable batteries.



Hong Li is a professor in Institute of Physics, Chinese academy of Science. His research interest include fundamental researches in batteries, such as transport of ions and electrons, size effect, interface phenomena, structure evolution as well as application researches, including high energy density Li-ion batteries using Si based anode, solid lithium batteries and their failure analysis. He is leading a CAS SPRP "Battery for EV" 5-year program and serve as a committee member for Advanced Energy in Ministry of Science and Technology of China since 2012.

decomposition.<sup>[9]</sup> Some NASICON-type glass ceramics are introduced as an attempt to establish a solid-state Li–O<sub>2</sub> batteries and inhibit Li dendrite during cycling.<sup>[10]</sup> Nonetheless, the huge interfacial resistances between electrolyte and electrode retard the electrons and ions transfer both at the anode and cathode. Also, the constructional design to enable oxygen diffusion for cathodes faces great challenges for solid electrolyte, making the solid-state Li–O<sub>2</sub> batteries still in their infancy.

As mentioned above, due to that Li–O<sub>2</sub> battery combines the two challenging electrodes, the development is hampered by significant hurdles associated with air cathode, electrolyte and Li-metal anode, none of which is approaching the commercialization. Presented problems such as poor cycling efficiency, limited cycle life, unsatisfactory specific capacity, and even safety concerns are induced by side reactions, electrolyte decomposition, sluggish kinetics, unstable Li metal interface and others, which demand to be solved before the application. Actually, pure oxygen is usually employed rather than air to avoid contamination and side reactions.<sup>[11]</sup> Consequently, understanding what occurs in the cell fundamentally and novel material development is crucial.<sup>[12]</sup>

Along with the exploration of Li–O<sub>2</sub> batteries, enormous papers concentrate on oxygen reduction in relevant electrolyte for cathode and the electrolyte stability.<sup>[13]</sup> A plenty of progresses have been made in this field to offer researchers a broad and deepened view of the Li–O<sub>2</sub> chemistry underpinning Li–O<sub>2</sub> batteries. Performance such as the reversibility of air cathode and cycle durability has been improved significantly.

Nonetheless, the stability of metallic Li anode is mostly unguaranteed when observing the integrated issues of these cell components systematically. As a necessary ingredient in Li–O<sub>2</sub> batteries, understanding and mastering the science and engineering behind the Li-metal anode are decisive towards a practical Li–O<sub>2</sub> battery.

### 3. Li–Metal Anodes for Li–O<sub>2</sub> Batteries

#### 3.1. Importance

Li-metal anode has been regarded as a “Holy Grail” for energy storage with extremely high energy density and the lowest reduction potential, which has a long history but still cannot deliver a satisfying performance.<sup>[9,14]</sup> Researches of Li-metal anode for Li–O<sub>2</sub> batteries is becoming increasingly urgent regarding the following reasons.

(i) Metallic Li is indispensable in Li–O<sub>2</sub> chemistry if to realize the promising capabilities of energy storage and has been utilized in all types of Li–O<sub>2</sub> batteries. Moreover, much excess Li metal is not welcome as a threefold excess Li results in much lowered specific energy of 1800 Wh kg<sup>-1</sup> compared to that of 3458 Wh kg<sup>-1</sup> for stoichiometric Li.<sup>[12]</sup> The volumetric energy is even more decreased according to the low density of Li metal. Nowadays, the cycling efficiency and life span of Li-metal anode are still far from satisfactory although plenty of excess Li metal is utilized to compensate for the Li consumption.

(ii) Improved cycling performance require a full picture of Li–O<sub>2</sub> battery and obey the law of the minimum. Hence the failure of Li-metal anode and the ion-transportation interface will indeed lead to degradation in battery efficiency and cycle life even the cathode remains intact.

(iii) Safety is the paramount for systems with high energy density. Li-metal anode is widely known for dendrite that formed during electrochemical depositions, resulting in serious safe hazards. This issue is even more serious in the Li–O<sub>2</sub> batteries with the addition of oxygen/water vapor crossover and severe electrolyte decomposition. Hence the Li-metal anode constitutes a significant component influencing Li–O<sub>2</sub> batteries.

#### 3.2. Challenges

Formidable challenges for Li-metal anode in a closed cell include the non-uniform deposition/dissolution, large volume changes, adverse reactions with electrolyte and increased interfacial resistances, many of which are owing to the formation and undesirable crack of solid electrolyte interphase (SEI) during cycling, as schematically shown in Figure 1. These

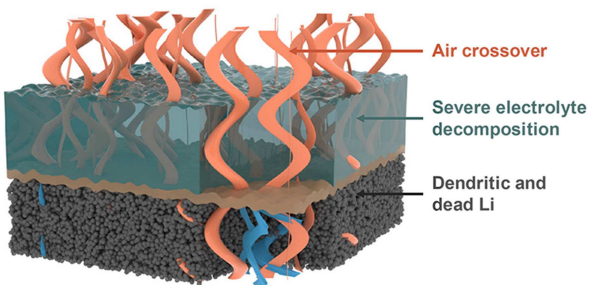


Figure 1. Challenges facing Li-metal anode in Li–O<sub>2</sub> batteries.<sup>[9]</sup> Reproduced and relabeled with permission from ref. [9]. Copyright (2019) Elsevier.

significant obstacles still exist in Li–O<sub>2</sub> batteries as electrolyte and reactive metallic Li are also employed.<sup>[14a]</sup> Furthermore, the semi-open Li–O<sub>2</sub> chemistry has proposed unique challenges and requirements for metallic Li, which are listed as follows.

(i) The chief problem for Li-metal anode in Li–O<sub>2</sub> batteries is the crossover of oxygen, water and other substances in the atmosphere.<sup>[15]</sup> As the air-breathing cathode is designed for continuous oxygen supply, the electrolyte and Li-metal anode is nearly open to the air, facilitating the corrosion of metallic Li to form ion-insulated Li salts (i.e., LiOH, Li<sub>2</sub>O), afterwards problems such as enlarged polarization and shortened cycle life occur. Accordingly, a protective strategy for Li-metal anode to resist air, especially oxygen and moisture, is of vital importance for battery operation.

(ii) Electrolyte decomposition and products from cathode hugely impact the stability of metallic anode in Li–O<sub>2</sub> batteries. During cycling, the redox mediators utilized for the catalytic reactions, generated intermediates such as radicals, and various side products not only interact with Li metal directly, also

accelerate electrolyte decomposition, resulting in severe interfacial degradation.<sup>[16]</sup> For instance, a certain amount of water will not only be transported to the metal anode surface, but also be generated due to the reaction of poly (vinylidene fluoride) (PVDF) binder, intermediates (i.e., LiO<sub>2</sub>), and liquid electrolyte.<sup>[8,17]</sup> Besides, traditional carbonate electrolyte in Li-ion batteries is too susceptible to avoid nucleophilic attack, making it gradually abandoned in Li–O<sub>2</sub> batteries. Novel electrolyte such as dimethyl sulfoxide (DMSO) and ionic liquid are promising,<sup>[18]</sup> but they still suffer from unstable interfacial property when contacting Li metal and decreased oxygen solubility, respectively. Thus, it is rewarding to develop a highly stable electrolyte regarding both electrodes and protect metallic Li from detrimental products.

(iii) The approaches for anode protections in Li-ion or Li–S batteries are proven difficult to become compatible with Li–air battery due to the Li–O<sub>2</sub> chemistry.<sup>[19]</sup> Carbonate-based electrolyte as well as the classical salt LiPF<sub>6</sub> in solid polymer, exhibits decomposition when access the moisture, leading to a rapid decay.<sup>[3,20]</sup> Hence identifying reactions on the metallic Li and unique solutions for anode protection is required.

Hence, the investigation and protection of Li-metal anode in Li–O<sub>2</sub> batteries is of urgent importance to improve the overall battery performance. In this review, various advanced characterization techniques over the past few years have been employed to understand the mechanism and fundamental issues of Li–O<sub>2</sub> batteries. Recent progresses on the characterizations of Li-metal anode based on advanced techniques are summarized. Characterization methods, testing conditions as well as the restrictions of these advanced techniques, ex-situ or in-situ, are discussed in the following part. Moreover, viable technologies and solutions towards practical Li–O<sub>2</sub> batteries are also forecasted in this review.

## 4. Characterization of Li–Metal Anodes

Advanced characterization techniques are necessary to uncover fundamental mechanism behind Li batteries. And the obtained in-depth insights further facilitate and guide the development of superior batteries. For Li-metal anode, various characterization techniques have demonstrated their importance in promoting the development of Li batteries. In the following section, we will briefly retrospect the challenges and characterizations of Li-metal anode, and then we will focus on the Li–O<sub>2</sub> batteries with case studies. By diverse techniques, insights related to morphological, constitutional, structural and interfacial information can be obtained.

### 4.1. Characterization of Li–Metal Anodes for Li–Metal Rechargeable Batteries

The incomparable advantages and the severe challenges of Li-metal anode aroused considerable research attention over the past years. Presently, it is widely accepted that the utilization of Li-metal anode is key to next generation of energy storage

devices beyond Li-ion batteries. Promising Li metal batteries were developed including Li–air batteries, Li–S batteries and other cathode type Li metal batteries. Cui, Zhang, Sohn, and McCloskey et al. have systematically reviewed the fundamental problems, characterization techniques and modification methods of Li-metal anode.<sup>[21]</sup> Briefly, Li-metal anode is hindered by safety and cyclability related issues. The challenges lie in the uncontrollable dendrite growth and low coulombic efficiency. Specifically, high reactivity, uneven deposition/stripping and large volume change are major obstacles in the way of Li-metal anode application.

Targeting at different scientific issues, diverse characterization tools can be utilized correspondingly. As for the dendrite growth, morphology characterization will be a most direct choice. However, dendrite growth involves characterizations with various spatial resolutions and characteristic scales expanding from micrometer to atomic distance. As a result, the combination of microscopic techniques including Optical Microscope (OM), Scanning Electron Microscope (SEM), Transmission Electron Microscope (TEM) may play a vital role. 3D morphology can be further probed by Atomic Force Microscope (AFM) and Transmission X-ray Microscope (TXM) with modest spatial resolution. Meanwhile, the dynamic evolution of Li dendrite further calls for characterizations with time resolution. And the nanoscale Li dendrite needs careful protection in case of artificial effect or pollution. Following these demands, designing morphology characterizations with in-situ and operando mode came into rapid development in the past years, which provide valuable insights into Li dendrite formation and evolution. On the other hand, the high reactivity of Li metal may well induce SEI formation, and the composition analysis of SEI layer becomes another vital topic. The complicated interface reaction makes the SEI layer a complex system consisting of organic and inorganic components. The identification of newly-formed phased relies on structural analysis, valence probe and functional groups assign, which can be realized by techniques including X-ray Diffraction (XRD), Fourier Transform Infrared Spectroscopy (FTIR), Raman Spectroscopy, Mass spectra, respectively. Furthermore, the radical evolution of SEI from surface to bulk requires characterizations with spatial resolution to figure out depth-related-evolution. X-ray Photoelectron Spectroscopy (XPS) analysis with depth resolved mode may well meet the requirement. As for SEI composition analysis, in-situ and operando characterizations are also an important part to ensure the reliability of ex-situ measurements and obtaining time-resolved composition change. On Li anode investigations, Zhang and Novák et al. have summarized and compared common characterization techniques including SEM/TEM, AFM/Scanning Probe Microscopy (SPM), Nuclear Magnetic Resonance (NMR), FTIR, XPS, Electron Energy Loss Spectroscopy (EELS), X-ray Absorption Near Edge Structure (XANES), Electrochemical Impedance Spectroscopy (EIS), etc.<sup>[21c,22]</sup> Cui further summarized advanced characterization techniques for Li-metal anode such as in-situ TEM, in-situ SEM, Scanning Transmission Electron Microscopy (STEM), operando synchrotron XRD, X-ray tomography and operando Magnetic Resonance Imaging (MRI).<sup>[21a]</sup> Readers are

encouraged to refer to relevant works for comprehensive information.

#### 4.2. Characterization of Li–Metal Anodes for Li–O<sub>2</sub> Batteries

Compared with conventional Li batteries with Li metal as anode, Li–O<sub>2</sub> batteries suffer consistent challenges as discussed above, i.e., Li dendrite formation and SEI growth. In the following paragraphs, the characterizations of Li-metal anode for Li–O<sub>2</sub> batteries are basically divided into two categories: one for morphology and microstructure investigations on Li anode and the other for chemical composition or bonding states analysis on SEI components. Note that Li–O<sub>2</sub> batteries present uniqueness compared with conventional batteries, where gas phase O<sub>2</sub> works as the cathode in semi-open battery structure. Such uniqueness further complicates electrochemical process of Li–O<sub>2</sub> batteries and requests special treatment in characterization, such as the approach of oxygen supply and the combination of characterization tool and the test battery. Possible demonstrations that can be referenced have been proposed by many researchers.<sup>[23–24,26,32–33,37,41b,43a,47]</sup> To provide an overview of the characterization of Li metal in Li–O<sub>2</sub> batteries, Figure 2 and Table 1 have summarized and compared the most common and powerful characterization techniques. In the following paragraphs, we will firstly discuss morphology and microstructure characterizations with various microscopies

as the main focus. By virtue of OM, SEM, TEM, and STEM such laboratory accessible techniques, Li-metal anode surface morphology can be well mapped out. With the increasing spatial resolution from OM to STEM, the comprehensive understanding of morphology features can be obtained from macro-size full scale down to micro even atomic scale. The utilization of AFM brings about high surface sensitivity, while synchrotron based TXM can present overall 3D morphology. The combination and comparison of various microscopies may well lead to full picture of electrode morphology. As for chemical composition analysis, XRD will be spearheaded for new phase identification due to its facile accessibility and specialty for bulk crystalline characterization. Following that, we will move on to three prevailing surface detection methods, i.e., XPS, FTIR, Raman with different working principles and sensitivity to fingerprinting various chemical environments. At the end of this section, NMR (MRI) and SIMS which can also achieve in-depth profile analysis are complemented with both composition and spatial resolution.

##### 4.2.1. Morphology and Microstructural Characterization of Li Surface

To detect the morphology characteristic of Li dendrite, electron microscopy is a most straightforward technique while OM is very suitable to quickly make a rough visualization. OM can directly monitor the macrostructure morphology change of anode surface and Li dendrite formation, Figure 3. With visible light as the probe mediate, the diffraction limit confined the spatial resolution of OM ~200 nm, which is a major hindrance for detailed and in-depth investigation.<sup>[35]</sup> However, the penetration depth of visible light in glasses does make OM a good choice for operando studies. Combined with a digital recording device, OM can record the evolution of Li morphology change in real time. As a comparison, both in-situ SEM and TEM are limited to the ionic liquid or solid-state electrolyte. Under these

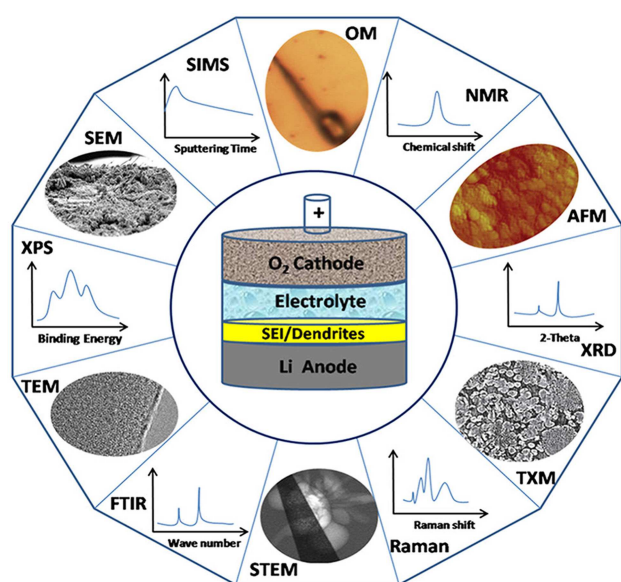


**Figure 2.** Most commonly used basic characterization techniques for Li-metal anode in Li–O<sub>2</sub> batteries. Morphology characterization techniques include six microscopy techniques i.e., OM,<sup>[27]</sup> SEM,<sup>[58]</sup> TEM,<sup>[24]</sup> STEM,<sup>[25]</sup> TXM,<sup>[26]</sup> AFM.<sup>[58]</sup> Chemical characterization techniques include six spectroscopy techniques i.e., XPS, FTIR, Raman, XRD, NMR, SIMS. The image of OM is reproduced with permission from ref. [27]. Copyright (2014) Elsevier. The images of SEM and AFM are reproduced with permission from ref. [58]. Copyright (2018) John Wiley and Sons. The image of TEM is reproduced with permission from ref. [24]. Copyright (2017) American Chemical Society. The image of STEM is reproduced with permission from ref. [25]. Copyright (2015) American Chemical Society. The image of TXM is reproduced with permission from ref. [26]. Copyright (2013) Springer Nature.

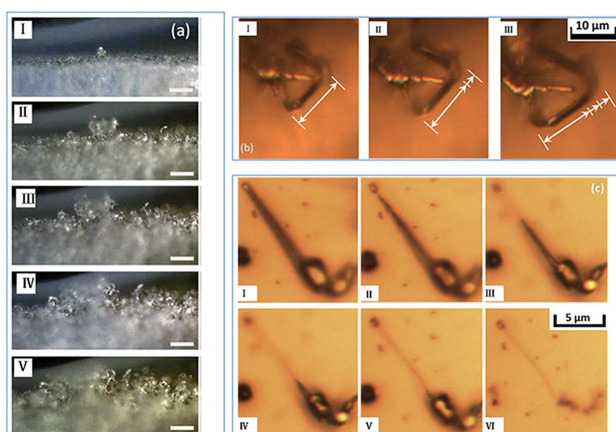


**Figure 3.** a) In-situ OM observation of Li dendrite formation.<sup>[28b]</sup> Reproduced with permission from ref. [28b]. Copyright (2015) Springer Nature. b), c) In-situ OM observation of the growth and electro-dissolution of Li dendrite.<sup>[27]</sup> Reproduced with permission from ref. [27]. Copyright (2014) Elsevier.

**Table 1.** Basic characterization techniques for Li-metal anode and corresponding fundamental understanding.

Technique	Function	Resolution	Applications	Advantages	Disadvantages
OM	Measure surface morphology	~0.2 um	A rough visualization of surface evolution; <sup>[27–28]</sup>	Quick and dynamic observation	Low resolution
SEM	Measure surface morphology and structure	5–10 nm	Analyze effects of different electrolytes on Li surface morphology; <sup>[29]</sup> Confirm Li anode structure design can mitigate dendrite; <sup>[30]</sup> Observe unexpected hollow structure dendrite; <sup>[31]</sup> Observe Li <sub>2</sub> O <sub>2</sub> morphology evolution; <sup>[32]</sup>	Large depth of field and wide magnification range	2D image and limited to surface
TEM	Measure surface morphology and crystallization	Less than 1 nm	Observe interface morphology evolution; <sup>[33]</sup> Observe Li electrochemical deposition behavior and SEI microstructure; <sup>[24]</sup>	Identify surface or edge microstructure	High quality requirements for samples
STEM	Identify surface morphology and component elements	Less than 1 nm	Evaluate the Li surface and the density of SEI; <sup>[34]</sup> Observe Li deposition/dissolution process; <sup>[25]</sup> Observe SEI and Li dendrite evolution; <sup>[34]</sup>	High resolution and high contrast	Limited to high vacuum and small detection area
AFM	Measure a true 3D surface profile	Less than 1 nm	3D surface morphology image; <sup>[23,35]</sup>	Atomic resolution	Limited by surface undulation and local area
TXM	Measure overall morphology	Down to 50 nm	Observe the evolution of Li dendrite; <sup>[36]</sup> Observe the evolution of a porous structured layer on Li surface; <sup>[37]</sup>	Non-destructive 3D imaging	Low resolution
XRD	Identify crystalline phases and crystallization	More than 100 nm	Investigate the evolution of Li electrode composition and structure under different charging and depth of discharge conditions; <sup>[26]</sup> Demonstrated the formation of LiOH and Li <sub>2</sub> CO <sub>3</sub> at Li surface; <sup>[38]</sup> Confirm the formation of LiOH on Li surface after cycled; <sup>[37]</sup>	Non-destructive, non-contact and high sensitivity	Limited to crystalline structure
XPS	Identify elements and chemical states	500 nm (spot size)	Identify surface layer composition and content; <sup>[23,30,39]</sup>	High sensitivity of ppm to elements	shallow detection depth of ~10 nm
FTIR	Identify polar molecular vibration	2–4 cm <sup>-1</sup>	Identify different functional groups and compositions <sup>[30,37,40,41]</sup> ; Observe evolution of the Li surface; <sup>[42]</sup>	High sensitivity of ppm to functional groups, strong signal and easy to measure	Limited to polar molecular structure and vulnerable to moisture interference
Raman	Identify non-polar molecular vibration	0.65–1.6 cm <sup>-1</sup>	Identify O–O vibrations; <sup>[43]</sup> Characterize the Li surface chemistry; <sup>[44]</sup> In-depth analysis along the Li/electrolyte interface; <sup>[45]</sup> Further characterize the composition of SEI; <sup>[46]</sup> Conform surface layer formed was inhomogeneous; <sup>[47]</sup>	High sensitivity of ppm to molecular vibration or rotation	Limited to non-polar molecular structure and weak signal and easy to be interfered by fluorescence scattering
NMR(MRI)	Fingerprint local chemical environment and probe surface morphology	Down to 0.08 mm	Observe the nucleation and growth of Li dendrite; <sup>[48]</sup> Identify surface layer structure; <sup>[39e]</sup>	High sensitivity of ppb and in-depth detection	Large error in quantitative analysis
SIMS	Identify composition and organic macromolecular structure	Down to 50 nm (Z direction)	Identify the composition of the Li surface; <sup>[49]</sup> Identify the composition of SEI in two different kind of electrolyte solvents; <sup>[50]</sup>	High sensitivity of ppm to all elements and depth profile analysis	Limited to known elements and planer resolution

circumstances, OM is a fine compromise for in-situ analysis compatible with liquid electrolyte.<sup>[27,28b]</sup> For Li–O<sub>2</sub> batteries, OM is still a suitable alternative to make a rough detection and the battery construction is simpler than other microscopy techniques.

To achieve even higher spatial resolution, SEM is another conventional technique to directly probe morphology information of the Li surface and dendrite.<sup>[51]</sup> The morphological change of Li can be vividly compared and presented upon various factors including different charge and discharge conditions, different electrolyte systems, or even different modification effects. Chen et al. reported a novel type solvent-in-salt electrolyte and investigated the effect of the electrolyte concentration on Li surface by SEM which demonstrated that a higher concentration can help suppress dendrite growth and volume change of Li anode.<sup>[29]</sup> Peng et al. designed a 3D cross-stacked carbon nanotube network anode for Li–O<sub>2</sub> batteries to

induce Li deposition and the SEM images of Li surface morphology after cycled confirmed the positive modification effect of such design.<sup>[30]</sup> Zaghib et al. conducted in-situ SEM on Li dendrite and unexpectedly found that the composition of Li dendrite is not pure Li metal as generally considered but carbide-based, Figure 4a,b. Such carbide dendrite in a Li-polymer battery has a hollow morphology and are harder than pure Li so it is easier to pierce the membrane.<sup>[31]</sup> Based on SEM, Li et al. reported an in-situ environmental scanning electron microscope (ESEM) investigation on a specially designed all-solid-state Li–O<sub>2</sub> battery and observed various morphologies such as sphere and film shapes of the discharge product Li<sub>2</sub>O<sub>2</sub> as well as their evolution during cycling Figure 4c,d.<sup>[32]</sup> Recently, Xia, Wang and Zhang et al. employed SEM to vividly highlight the severe corrosion and dendrite formation problems of Li-metal anode in Li–O<sub>2</sub> batteries and reported a series of solutions such as composite anode host, multifunctional ionic

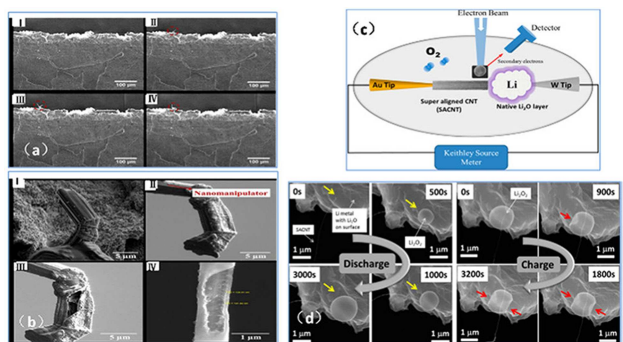


**Figure 4.** a), b) SEM images of carbide dendrite in Li-polymer batteries.<sup>[31]</sup> Reproduced with permission from ref. [31]. Copyright (2018) American Chemical Society. c), d) The set up and detection images of in-situ ESEM for solid state Li–O<sub>2</sub> batteries.<sup>[32]</sup> Reproduced with permission from ref. [32]. Copyright (2014) American Chemical Society.

liquid and in-situ surface protective layer.<sup>[52]</sup> Xia et al. innovatively employed RuO<sub>2</sub>-CNTs composite as a special Li-metal anode host in Li–O<sub>2</sub> batteries and confirmed its excellent dendritic inhibition effect by SEM.<sup>[52a]</sup> Wang et al. reported the severe corrosion and dendrite formation problems of Li-metal anode in Li–O<sub>2</sub> batteries by SEM and proposed a multifunctional ionic liquid electrolyte to overcome these problems.<sup>[52b]</sup> Zhang et al. studied the corrosion of Li-metal anode in Li–O<sub>2</sub> batteries caused by oxygen and moisture by SEM and firstly demonstrated the excellent protective effect of tetraethyl orthosilicate as a kind of electrolyte additive.<sup>[52c]</sup>

To gain more insights into microstructure of Li dendrite, TEM is a prevailing choice with even higher resolution down to atomic scale. With the combination of affiliated Selected Area Electron Diffraction (SAED), Electron Energy Loss Spectroscopy (EELS) or Energy Dispersive Spectrometer (EDS), the chemical composition information of Li dendrite or SEI layer can be well obtained.<sup>[53]</sup> For Li–O<sub>2</sub> batteries, TEM is often utilized to characterize the cathode and the discharge products.<sup>[54]</sup> With the hermetic electrochemical liquid cells successfully fabricated to satisfy the in-situ TEM characterization, the chance of observing the morphology and microstructure change in a liquid Li–O<sub>2</sub> battery is increasing.<sup>[53,55]</sup> Cui et al. conducted in-situ TEM to observe the deposition of Li within the hollow carbon nanospheres and suggested the interface engineering is of much significance to promote Li-metal anode for new batteries such as Li–S and Li–O<sub>2</sub> batteries, Figure 5a.<sup>[33]</sup>

Based on TEM, in-situ electrochemical transmission electron microscopy (ec)-TEM is gradually developed and it can provide external conditions to control potential together with record current so it can visualize the process of the Li surface evolution. In addition to STEM, Unocic et al. also utilized such ec-TEM on a three-electrode cell with gold as working electrode and LiPF<sub>6</sub>-EC:DMC as electrolyte. They reported that the dendritic SEI had been formed at the surface before the Li deposition and it would maintain after Li electro-dissolution.<sup>[56]</sup> Despite the different systems, such characterization technique should be taken into consideration for Li–O<sub>2</sub> batteries. Kourkoutis et al. proposed a novel cryo-STEM technique

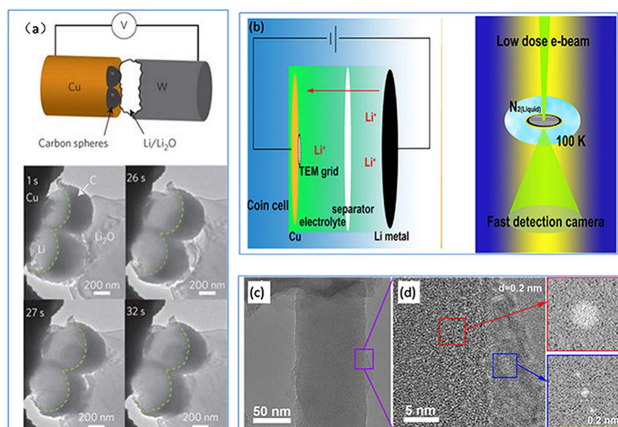


**Figure 5.** a) In-situ TEM cell and images of Li deposition process.<sup>[33]</sup> Reproduced with permission from ref. [33]. Copyright (2014) Springer Nature. b) Schematic cell and cryo-TEM for characterization. c), d) Cryo-TEM images of deposition of Li.<sup>[24]</sup> Reproduced with permission from ref. [24]. Copyright (2017) American Chemical Society.

together with cryo-TEM to systematically characterize Li dendrite and SEI in Li metal batteries.<sup>[57]</sup> Cryo-electron microscope has a unique advantage of vitrifying the liquid electrolyte and preserving the native states of the interphase. Coincidentally, Meng et al. also conducted the cryo-TEM to analyze the Li electrochemical deposition behavior and SEI in a Li battery, Figure 5b,c,d.<sup>[24]</sup> They found the amorphous structure of the deposited Li and there was crystalline LiF in SEI. All such detailed and valuable information suggests the huge advantage of cryo-electron microscope. Although not yet practiced, TEM based advanced characterization such as ec-TEM and cryo-TEM could be introduced for Li–O<sub>2</sub> systems.

Chemically sensitive STEM can be also applied to evaluate the Li surface and the density of SEI Figure 6.<sup>[34]</sup> The good understanding of the Li depositing and dissolving process can be conducted by in-situ STEM to image the first few cycles of Li

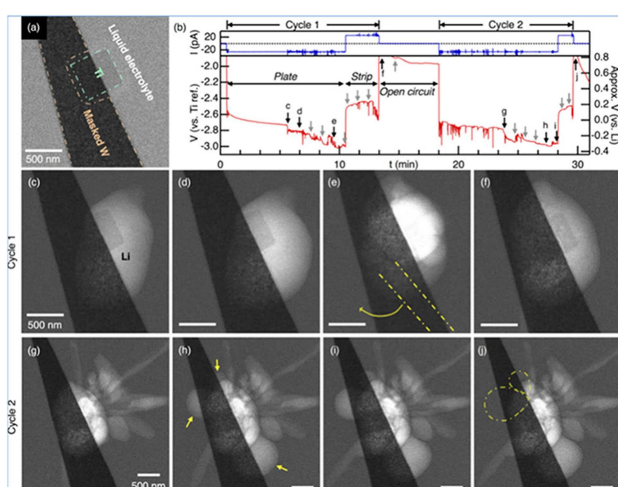


**Figure 6.** STEM images collected over the Li electrodeposition and stripping process in two cycles.<sup>[25]</sup> Reproduced with permission from ref. [25]. Copyright (2015) American Chemical Society.

electro-deposition/dissolution in liquid aprotic electrolyte at submicron resolution.<sup>[25]</sup> Unocic et al. investigated the mechanism of SEI and Li dendrite evolution at the interface between Li metal and standard liquid electrolyte ( $\text{LiPF}_6$  in EC:DMC) by in-situ STEM combined with quantitative electrochemically controlled potential conditions.<sup>[34]</sup> They detected the phase transformation and reported that the density of SEI formed under such condition is twice than that of electrolyte. Besides, they observed the nucleation sites as well as the growth of Li dendrite which explained the strong power of chemical element sensitive STEM combined with accurate electrochemical condition control. Similarly, the application of STEM in  $\text{Li}-\text{O}_2$  batteries will provide valuable information when the experimental set-up can be successfully designed.

By monitoring the micro strain on cantilever, AFM is another direct probe of the nanoscale surface morphology of Li anode with high resolution of atomic scale.<sup>[37]</sup> Compared with electron microscopy, AFM is more compatible with insulating samples or insulating organic components, and the morphology achieved from AFM provides three dimensional features of sample surface. Besides, AFM is a non-destructive probe which can well maintain the practical feature of Li dendrite without damage effect and the change of volume or morphology during Li deposition and extraction can be detected by in-situ AFM. Zhang et al. utilized in-situ AFM in a  $\text{Li}-\text{O}_2$  battery to characterize the Li surface roughness under different charging potentials and the roughness data results demonstrated that the electrolyte decomposition and Li plating were two main sources for surface film roughness evolution, Figure 7.<sup>[58]</sup>

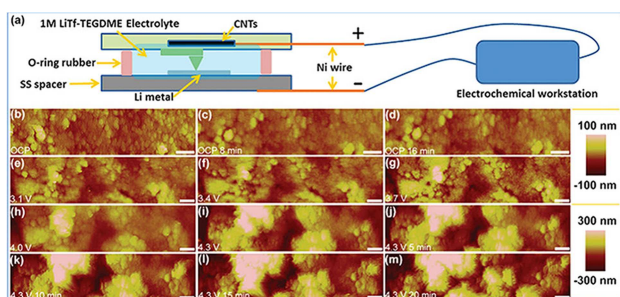


**Figure 7.** a) Schematic diagram of the setup of in-situ AFM. b)-m) AFM images of Li metal surface at different conditions.<sup>[58]</sup> Reproduced with permission from ref. 58. Copyright (2018) John Wiley and Sons.

In addition to the lab-based characterizations accessible by most research groups, advanced characterizations based on synchrotron facility also provide powerful techniques for Li dendrite characterization. TXM and X-ray tomography are emerging novel imaging techniques that can provide valuable detailed internal structure information.<sup>[26]</sup> By scanning focused probe beam across samples within TXM and X-ray tomography, 2D or 3D morphology can be mapped out or reconstructed within non-destructive mode. Manke et al. utilized in-situ synchrotron TXM to study the change of Si anode and suggested that the volume change could be quantified.<sup>[59]</sup> Thoughtfully, such technique can be applied to Li anode as

well. Synchrotron based hard X-ray micro-tomography has been applied to observe the evolution of Li dendrite in symmetric Li–polymer batteries.<sup>[36]</sup> As for  $\text{Li}-\text{O}_2$  batteries, Manke et al. conducted in-situ synchrotron X-ray tomography on Li-metal anode and confirmed the formation and evolution of a porous structured layer on Li surface, Figure 8.<sup>[37]</sup> Besides

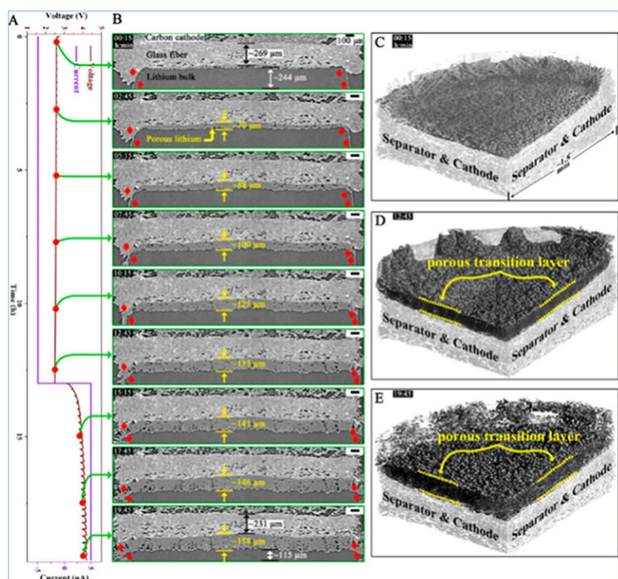


**Figure 8.** In-situ synchrotron X-ray tomography of Li-metal anode during the first discharge-recharge process.<sup>[37]</sup> Reproduced with permission from ref. [37]. Copyright (2019) American Chemical Society.

synchrotron based X-ray tomography, Neutron imaging was also utilized to characterize the internal morphology of the  $\text{Li}-\text{O}_2$  batteries after different cycle numbers. Note that the spatial resolution of these techniques still needs further improvement to be competitive with electron microscopy. Meanwhile the data collection and processing efficiency also awaits significant advance to make these novel tools accessible for wider investigations.

In addition to these common microscopy devices, novel microscopy such as Laser Scanning Confocal Microscopy (LSCM) can also be used to observe the Li dendrite.<sup>[60]</sup> Homma et al. conducted in-situ LSCM to investigate the Li dendrite on Ni substrate in a  $\text{LiClO}_4$ -PC electrolyte system. The operando Electron Paramagnetic Resonance Spectroscopy (EPRS) can also be applied to study Li dendrite in real-time and under working conditions. This technique provides time-resolved semi-quantitative information on mossy Li and dendrite formation during electrochemical cycling.<sup>[61]</sup>

It is worth noting that microscopy techniques listed above exhibits distinguished spatial resolutions due to different operation mechanism. Within OM, SEM, TEM, AFM, TXM etc., the spatial resolution ranges from micrometer down to atomic scale. Considering the complexity of Li dendrite related issues within various length scales, the combination of diverse microscopic techniques exhibits particular advantages in providing comprehensive and in-depth understandings of Li dendrite

formation and evolution. Moreover, the development of in-situ and operando characterization within conventional microscopy techniques may further add up to the full picture of Li dendrite related issues.

Moreover, NMR (MRI) is also an important characterization technique to monitor Li dendrite growth. It works on detecting the chemical bonding or atomic environment and gradually becomes another effective technique to observe the nucleation and growth of Li dendrite.<sup>[62]</sup> Bhattacharyya and Grey et al. conducted in-situ NMR and successfully observed the process of Li dendrite formation at the surfaces between Li and different electrolytes.<sup>[48]</sup> For Li dendrite characterization, it is better to quantify the formation and growth process to quantitatively describe the conditions. Unfortunately, common electron microscopy or optical microscopy only provide morphology information that is not accurately quantified. Grey et al. employed in-situ NMR spectroscopy on Li dendrite characterization which can achieve quantification of the Li microstructures (cover both dendrite and moss).<sup>[48]</sup> The basic principle can be simply interpreted as the signal of Li microstructures is in direct proportion to their volume or mass but the bulk Li signal is only proportional to its area not volume so the two signals can be separated from each other. Rathke et al. once used NMR to characterize Li dendrite on carbon anode and got very clear and intuitive image results, Figure 9a.<sup>[63]</sup> Grey et al. have also utilized <sup>7</sup>Li MRI in Li bag cells to determine the location of Li microstructure during charging process at a resolution of dozens micron by comparing the cell MRI images of before and after charging process, Figure 9b,c.<sup>[62]</sup> Proper battery construction design will make it suitable for Li anode in Li–O<sub>2</sub> batteries.

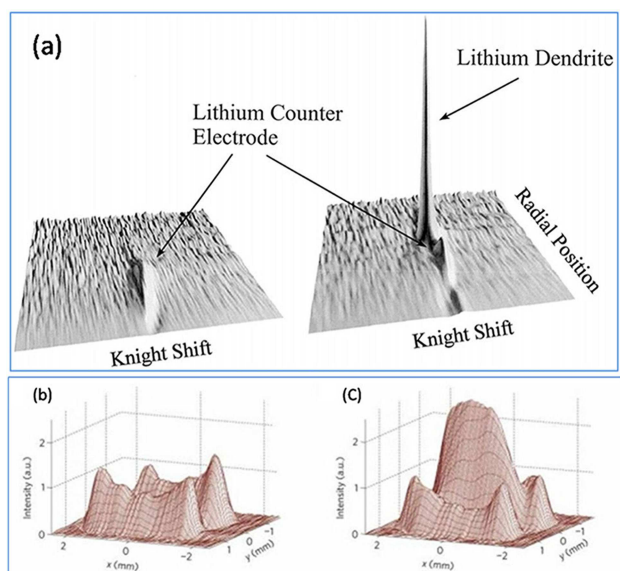


**Figure 9.** a) <sup>7</sup>Li NMR images of the Li dendrite formed on a hard carbon electrode.<sup>[63]</sup> Reproduced with permission from ref. [63]. Copyright (2000) Elsevier. b), c) <sup>7</sup>Li MRI of Li microstructure formation in Li bag cells in pristine state and charged state.<sup>[62]</sup> Reproduced with permission from ref. [62]. Copyright (2012) Springer Nature.

#### 4.2.2. Chemical Composition or Bonding States Analysis on SEI Components

The exploration of the chemical composition of SEI layer and its evolution is of vital significance to the long-term cycle stability of Li–O<sub>2</sub> batteries. And the chemical constitution analysis relies on characterization techniques that are sensitive to the crystal structure, chemical composition, atomic bonds, elemental valence states etc.

With new chemical phases formation in SEI layer, XRD is a most commonly used and powerful tool to detect the material phase and its evolution. XRD patterns can identify the newly formed phase as well as the degree of crystallization by Rietveld refinement. Wagemaker et al. have successfully conducted operando X-ray diffraction to reveal a two-stage process of oxygen evolution reaction in a Li–O<sub>2</sub> battery.<sup>[64]</sup> Not only in Li–O<sub>2</sub> batteries, in-situ and operando XRD was also well utilized in Li–S batteries.<sup>[65]</sup> In addition to cathode side,<sup>[66]</sup> XRD can also characterize Li-metal anode. Typically, a synchrotron XRD ( $\mu$ -XRD) technique with spatial and temporal resolution was conducted to investigate the evolution of Li electrode composition and structure under different charging and depth of discharge conditions. The schematic of the set-up is shown as below. Liu et al. conducted the in-situ  $\mu$ -XRD and directly monitored the evolution of Li anode during operating including the phase transformation from Li to LiOH and the thickness increase of LiOH as cycle numbers increased which may be the reason for the failure of the Li–O<sub>2</sub> cell using LiCF<sub>3</sub>SO<sub>3</sub>/TEGDME electrolyte, Figure 10.<sup>[26]</sup> Amine et al. investigated the effect of the contaminant O<sub>2</sub> at Li anode with in-situ XRD and ex-situ FTIR in an ether-based electrolyte (tetraglyme, TEGDME) Li–O<sub>2</sub> battery. The XRD patterns and FTIR spectra demonstrated the formation of LiOH and Li<sub>2</sub>CO<sub>3</sub> at Li surface.<sup>[38]</sup> Recently, Manke et al. utilized XRD and confirmed the formation of LiOH on Li surface after cycled in a Li–O<sub>2</sub> battery.<sup>[37]</sup>

Although XRD may well characterize the periodic lattice and identify new phases, this technique is limited to detecting crystallized structure and insensitive to amorphous phases that widely distribute in SEI. Spectroscopic techniques including XPS, FTIR, Raman and XAS is very sensitive to local chemical environment changes with elemental resolution, which is suitable for composition analysis of both crystal and amorphous phases. Some spectroscopic techniques can be further used in quantitative analysis, which is beneficial to detailed analysis on SEI components evolution upon cycle.

XPS is a most popular technique to distinguish and analyze the chemical environment and oxidation states of the key elements with high sensitivity. With XPS spectra fitting, quantitative or quasi-quantitative information of each chemical component can be further obtained, which has been widely utilized in previous works. Aurbach et al. investigated the Li surface species quantitatively by XPS and the unique detection of Li–C bond which was a key SEI component and could not be analyzed by other previous spectroscopic tools, demonstrating the unique advantage of XPS.<sup>[67]</sup> XPS is also a powerful technique to investigate the stabilization effect of redox mediators, electrolyte additives and surface coating layer on Li-

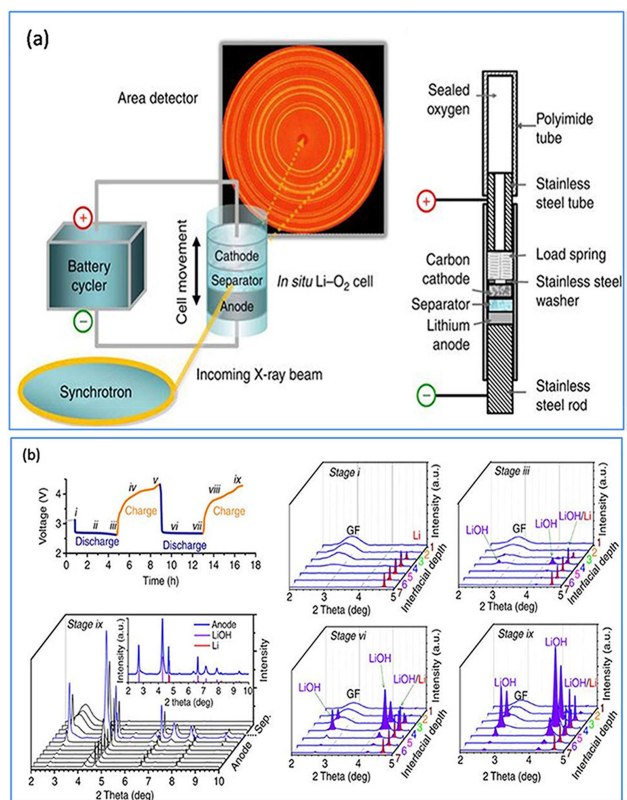


**Figure 10.** a) The experimental set-up of the operando  $\mu$ -XRD and Li–O<sub>2</sub> cell schematic design. b) Voltage profile and operando XRD patterns of Li-metal anode.<sup>[26]</sup> Reproduced with permission from ref. [26]. Copyright (2013) Springer Nature.

metal anode in Li–O<sub>2</sub> batteries.<sup>[39a,b,d-f,68]</sup> The modification effect of the 3D cross-stacked carbon nanotube network Li–O<sub>2</sub> anode proposed by Peng et al. was also examined by XPS. They analyzed the differences of SEI using the new Li anode and the one after cycled. The results showed that the contents of LiOH and Li<sub>2</sub>CO<sub>3</sub> are evidently decreased when the Li anode is modified which corresponds to the enhanced performance.<sup>[30]</sup> Remarkably, Zhang et al. utilized XPS to characterize the composition of the Li surface under 4.3 V potential and 10 minutes long pre-charge condition in a Li–O<sub>2</sub> battery. They analyzed the causes of each new emerging chemical bonding and confirmed that the surface layer are formed by both solvent and salt anions decomposition, Figure 11.<sup>[58]</sup> Park et al. used XPS to confirm the protective effects of a composite coating layer on Li-metal anode in Li–O<sub>2</sub> batteries by comparing the SEI composition of protected Li anode and unprotected one.<sup>[39g]</sup> It is worth mentioning that the shallow escape depth of emitted electrons ~3 nm has confined XPS to a surface layer analysis tool. With low energy Ar etching or changing incident X ray energy, the depth profile information can be achieved from XPS. Moreover, X-ray irradiation in XPS may further raise doubts on slight beam damage effect or potential artificial effect. Careful sample preparation and proper treatment process will be necessary to mitigate such side effects and achieve convincing results.

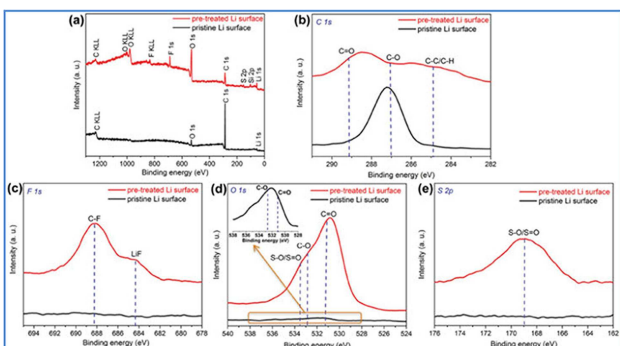


**Figure 11.** XPS spectra of the pre-charging treated Li-metal anode surface and the pristine Li metal surface.<sup>[58]</sup> Reproduced with permission from ref. [58]. Copyright (2018) John Wiley and Sons.

FTIR is another powerful tool for Li–O<sub>2</sub> batteries including Li surface characterization, with particularly advantage in identifying different functional groups and compositions.<sup>[30,37,41a,e]</sup> Aurbach et al. proposed the possible composition of the Li surface and some possible reactions between Li and electrolyte according to the FTIR results. With further research, in-situ FTIR were developed to monitor the evolution of the Li surface.<sup>[42]</sup> Slightly regrettably, it can only detect the functional groups or components with infrared activity. Thus, XPS is often cooperated with FTIR to get more complete and detailed information. For example, Aurbach et al. concluded the components of SEI formed between Li-metal anode and electrolyte mainly contain Li<sub>2</sub>O, LiOH, LiF, Li<sub>2</sub>CO<sub>3</sub>, lithium alkylcarbonate and hydrocarbons based on XPS and FTIR together.<sup>[69]</sup> Manke et al. suggested the failure the Li–O<sub>2</sub> battery caused by the formation of Li<sub>2</sub>CO<sub>3</sub> and LiOH after cycled by FTIR.<sup>[37]</sup> Peng et al. also employed FTIR to confirm the effect of the 3D cross-stacked carbon nanotube network Li–O<sub>2</sub> anode and the FTIR results showed that the designed anode is much less contaminated than pristine anode.<sup>[30]</sup> Specifically, Polarization Modulated Infrared Reflection Absorption Spectroscopy (PM-IRRAS), as a derived technique from FTIR, should also be taken into consideration when characterize the composition especially carbonate and hydroxide species of Li surface.<sup>[41c,d]</sup> Wohlfahrt-Mehrens et al. investigated the effects of O<sub>2</sub> and high salt concentration in the DMSO based electrolyte in Li–O<sub>2</sub> batteries and reported the absence of OH vibrations in the FTIR spectra of the cycled Li anode which demonstrated the un-decomposition of DMSO, confirming the stabilization effect of O<sub>2</sub> and high salt concentration, Figure 12.<sup>[41b]</sup>

As a complementary tool to FTIR that operates upon infrared dipole transition, Raman spectroscopy relies on the inelastic scattering of monochromatic light to detect the vibrational, rotational, and other low-frequency modes of samples. Compared with FTIR, Raman spectra is good at characterizing the center-asymmetric molecular skeleton that is dipole silent in FTIR. A most significant example is the probe of O–O bond which are directly associated with the reaction products over the charge-discharge process in Li–O<sub>2</sub> batteries. As a major reaction product, the characterization of Li<sub>2</sub>O<sub>2</sub> is key to understand the reaction mechanism. While the O–O bond

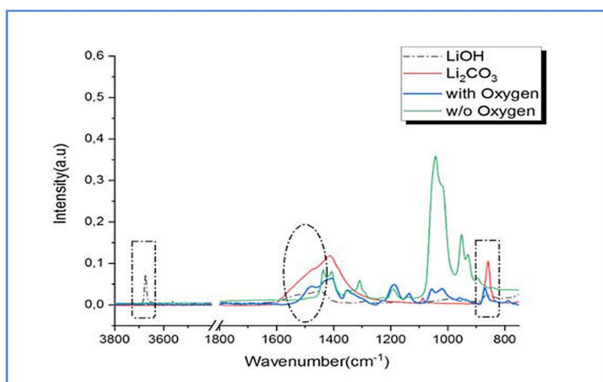


**Figure 12.** FTIR spectra of the Li-metal anode cycled in 3 M LiTFSI/DMSO under two oxygen flow conditions.<sup>[41b]</sup> Reproduced with permission from ref. [41b]. Copyright (2018) John Wiley and Sons.

exhibits nonpolar feature, Raman spectroscopy can uniquely identify the discharge products by detecting O–O vibrations while XPS or FTIR cannot.<sup>[43]</sup> On the other hand, laser in visible range is typically used as the irradiation source in Raman spectroscopy, this feature makes Raman particularly compatible for in-situ and operando investigation compared with FTIR and XPS. At early time, it was a main in-situ technique to characterize the Li surface chemistry in Li batteries.<sup>[44]</sup> The set-up of an in-situ Raman spectroscopy for characterizing Li–O<sub>2</sub> batteries is shown as below, Figure 13.<sup>[43a]</sup> In addition to normal Raman

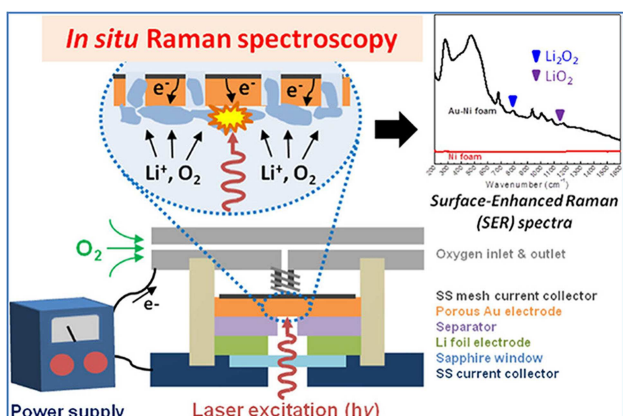


**Figure 13.** Li–O<sub>2</sub> cell schematic for in-situ Raman spectroscopy.<sup>[43a]</sup> Reproduced with permission from ref. [43a]. Copyright (2015) John Wiley and Sons.

spectroscopy, Confocal Raman Microspectrometry (CRM) is a novel technique and possesses great advantage for in-depth analysis along the Li/electrolyte interface.<sup>[45]</sup> Surface Enhanced Raman Spectroscopy (SERS) is another good choice to further characterize the composition of SEI.<sup>[46]</sup> In addition, operando SERS is also utilized for cathode material in Li–O<sub>2</sub> batteries.<sup>[70]</sup> Based on Raman spectroscopy, a newly developed Shell Isolated Nanoparticles for Enhanced Raman Spectroscopy (SHINERS) technique was conducted on Li-metal anode discharged in an oxygen saturated DME electrolyte and the results

showed that the surface layer formed during discharge was inhomogeneous due to the absence of Li<sub>2</sub>C<sub>2</sub> species which usually formed by laser decomposition.<sup>[47]</sup>

Besides these lab-based spectroscopic techniques, synchrotron based XAS is a significant complementary. XAS operates on the electronic transitions from core initial states to final states in continuum, following quantum mechanical selection rules. Due to the local geometric and electronic structural sensitivity, XAS is commonly used to fingerprint material change with high sensitivity. The extremely high flux of synchrotron facility further empowers XAS in monitoring imperceptible variations, while data collection in different modes provide the spectra contrast with various probing depth. For Li–O<sub>2</sub> batteries, XAS has been used to identify the oxidation state change and surface composition difference at cathode side.<sup>[54a,71]</sup> Yang et al. utilized XAS on various element redox couples in a lithium- and manganese-rich (LMR) layered material (Li<sub>1.2</sub>Ni<sub>0.15</sub>Co<sub>0.1</sub>Mn<sub>0.55</sub>O<sub>2</sub>) to investigate the fundamental mechanism of voltage fade and strictly proved that the consecutive reduction of the valence states of the transition metal elements and the oxygen release were main causes for the voltage fade.<sup>[62]</sup> Yet, its application on Li-metal anode for Li–O<sub>2</sub> batteries has not been reported. Toney et al. conducted XAS on Ge anode to study the influence of charge and discharge rate on Ge phase transformation during cycling.<sup>[72]</sup> And their results provide much valuable information and guidance in terms of improving the anode capacity retention and cycling stability. Such application would be suitable for Li-metal anode too.

As mentioned above, MRI can be utilized to visualize Li dendrite and quantitatively record the microstructure evolution. Besides observing anode material such as graphite and silicon,<sup>[73]</sup> it can as well be utilized to identify the discharge products for Li–O<sub>2</sub> batteries and it is demonstrated that the electrolyte composition can determine the discharge products generated at cathode side.<sup>[74]</sup> Grey et al. introduced LiI additive in Li–O<sub>2</sub> batteries to change the discharge product from Li<sub>2</sub>O<sub>2</sub> to LiOH and they conducted NMR to reveal the redox process mechanism.<sup>[75]</sup> As showed below, it is convenient to identify the discharge products and monitor the electrochemical process, Figure 14a,b,c. In contrast, the research about its application on Li surface characterization is seldom reported perhaps due to the characterization difficulty. Lee et al. conducted ex-situ NMR on cycled Li-metal anode in an DMA electrolyte under two different protective conditions and provided valuable information about the decomposition of the electrolyte, Figure 14d.<sup>[39e]</sup> Obviously, NMR/MRI are outstanding techniques which can provide both morphology and chemical composition information.

In contrast to the above-mentioned non-destructive techniques, mass spectra is a distinguished type of characterization method which split samples into molecular pieces for composition analysis with high specificity and high sensitivity. Secondary Ion Mass Spectrometry (SIMS) is an advanced surface characterization technique to reveal the chemical composition of real surface or near surface which is far from normal elemental analysis. It will be an accurate tool with sensitivity of

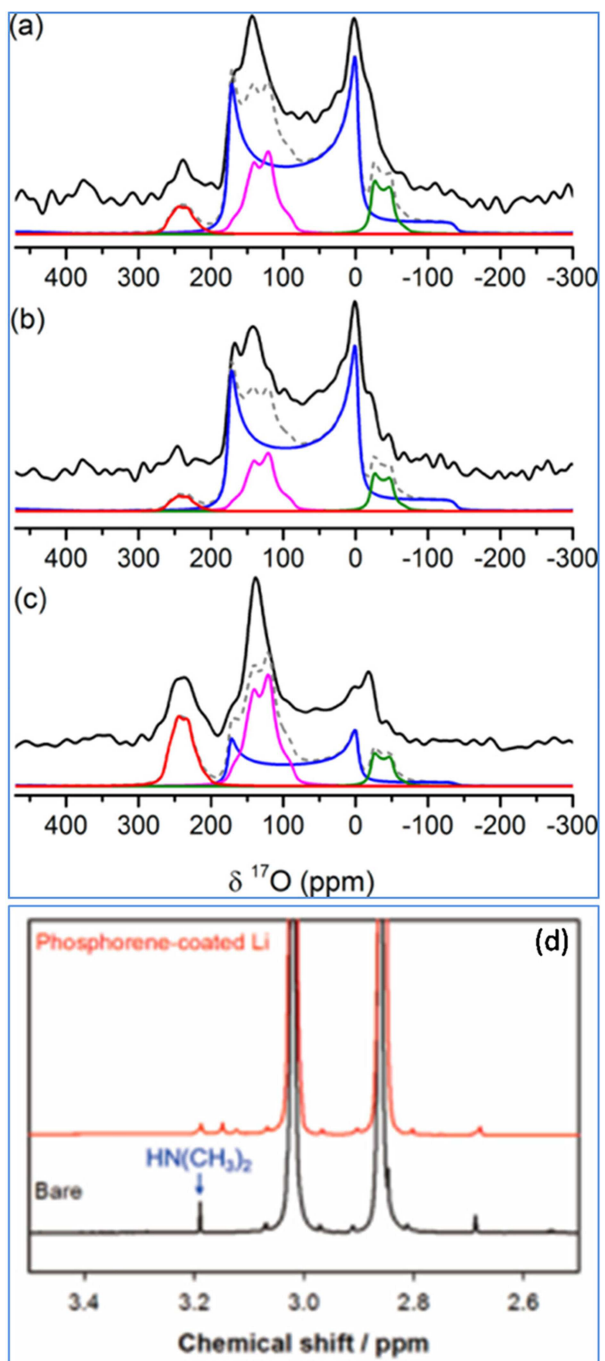


**Figure 14.** a, b, c) Identifying Li–air battery discharge products using  $^{17}\text{O}$  NMR.<sup>[76]</sup> Reproduced with permission from ref. [76]. Copyright (2013) American Chemical Society. d) NMR of the bare and phosphorene-protective Li metal after cycled.<sup>[39e]</sup> Reproduced with permission from ref. [39e]. Copyright (2018) American Chemical Society.

ppm even ppb level to identify the composition of Li surface no matter organic or inorganic including all elements. Nazri and Muller et al. studied the composition of the Li surface by SIMS and the results suggested the ingredient of polycarbonate, partially chlorinated hydrocarbon polymer and Li salt.<sup>[49]</sup> Scrosati et al. performed SIMS on Li– $\text{O}_2$  batteries cathode to confirm the reversible formation of  $\text{Li}_2\text{O}_2$ , Figure 15a.<sup>[77]</sup> In addition, SIMS has another advantage of depth analysis,

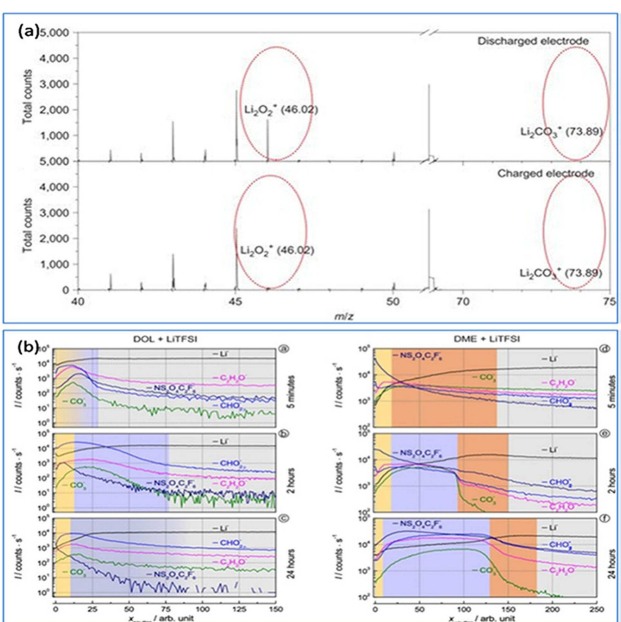


**Figure 15.** a) SIMS spectra of the oxygen cathode at fully discharged and fully charged states.<sup>[77]</sup> Reproduced with permission from ref. [77]. Copyright (2012) Springer Nature. b) SIMS depth profiles of SEI fragments from two kind of electrolyte solvents.<sup>[50]</sup> Reproduced with permission from ref. [50]. Copyright (2017) Electrochemical Society.

Figure 15b.<sup>[50]</sup> Janek et al. combined SIMS and XPS to identify the composition of SEI in two different kinds of electrolyte solvents. The capability of depth analysis of SIMS can well make up for the thin range limit of XPS.

Chromatographic and mass spectrometry characterization techniques such as Decomposition Mass Spectroscopy (DMS), Gas Chromatography-Mass Spectrometry (GC-MS) and Ion Chromatography (IC), Matrix-assisted Laser-desorption Ionization Time-of-Flight (MALDI-TOF) mass spectrometry<sup>[78]</sup> may also help to analyze the composition of the Li surface. Kominato et al.<sup>[79]</sup> and Ota et al.<sup>[80]</sup> conducted such techniques to characterize the Li surface film and analyze the composition. They are also very suitable for Li– $\text{O}_2$  batteries.

Except for the relatively common techniques as mentioned above, there are some other characterization techniques for Li– $\text{O}_2$  batteries analysis such as Sum Frequency Generation Vibrational Spectroscopy (SFG),<sup>[81]</sup> Scanning Vibrating Electrode Technique (SVET),<sup>[82]</sup> Chromatographic and mass spectrometry characterization techniques.<sup>[79–80]</sup> Other electrochemical techniques such as galvanostatic cycles<sup>[83]</sup> are also used to indirectly analyze Li dendrite. Balsara et al. observed the sharp drop of the oscillating voltage in a symmetric Li cell which reflects the growth of Li dendrite.<sup>[83]</sup> In-situ scanning vibrating electrode technique is introduced to analyze the electric field at Li surface as a new powerful type of characterization.<sup>[82]</sup> The electric field can well describe the formation and growth of Li dendrite and it is formed by the concentration gradient and ionic heterogeneous distribution caused by polarization. Unfortunately, the scanning step need to be further reduced to precisely measure the electric field distribution at Li surface. Following the extensive and continuous research efforts worldwide, many

progresses have been achieved on Li anode evolution upon reversible transitions. However, it is necessary to underline that each characterization technique relies on specific working principles and reflects sample information from certain perspectives. As a result, the combination of diverse characterization methods is essential to provide a full and comprehensive picture on the Li anode related procedures. Generally, spatial resolution is firstly taken into consideration when choosing microscopes. Besides, FTIR and Raman are complementary in terms of molecular polarity, XRD and TEM can work together to obtain complete lattice structure information including both bulk and surface phase, shallow depth detective technique such as XPS can be combined with SIMS or NMR to achieve in-depth detection, TXM and XAS are good partners to reveal the evolution process of internal morphology and chemical states.

## 5. Strategies for Li–Metal Anode Protection in Li–O<sub>2</sub> Batteries

Based on the fundamental insights obtained from various characterizations and relatively systematic improving solutions for Li metal battery without exposure to air, Li-metal anode modification and performance optimization strategies can be proposed correspondingly. In this section, the research progresses of stabilizing Li-metal anode in Li–O<sub>2</sub> batteries are reviewed from Li anode inside out to full battery encapsulation. Undoubtedly, further development should pay more attention to the integration and optimization of different solutions to prosper Li–O<sub>2</sub> batteries.

### 5.1. Anode Structure Design

In view of the highly reactive Li metal, the most direct strategy is to replace it. Based on such consideration, Li ion oxygen battery (LIOB) with intercalation materials or alloys as the anode was reported. Some steady Li-ion battery electrode materials were first applied to Li–O<sub>2</sub> batteries, including: LiFePO<sub>4</sub>,<sup>[84]</sup> Li<sub>4</sub>Ti<sub>5</sub>O<sub>12</sub>,<sup>[85]</sup> and so on. Although these alternative anode materials indeed mitigate related issues resulting from the employment of Li metal, this sacrifices the superior energy density of the Li–O<sub>2</sub> batteries. In recent years, there has been an increasing amount of literature on alloying strategy as a compromise. As indicated in Figure 16a, Kim, Yang, and co-workers applied alloy anode by the lithiation of aluminum foil in the EC/DEC electrolyte, which forms a durable SEI on the anode surface simultaneously.<sup>[86]</sup> Combining a Li<sub>2</sub>O<sub>2</sub>-preloaded oxygen cathode and a Nafion membrane as the oxygen barrier, the capacity of LIOB with the pre-lithiated aluminum anode maintains over 100 cycles without obvious decline and delivers a maximum energy density of 1178 Wh kg<sub>cathode</sub><sup>-1</sup> at a current density of 100 mA g<sup>-1</sup>. In another study, Hassoun et al.<sup>[87]</sup> investigated the feasibility of employing lithiated silicon-carbon anode in Li–O<sub>2</sub> batteries. In spite of the poor cycle life, the

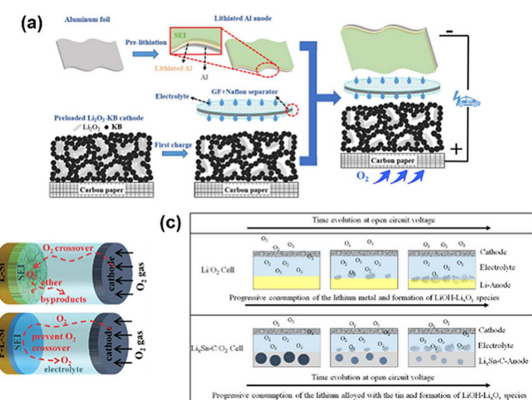


**Figure 16.** a) Assembly route for LIOB with a lithiated aluminum anode.<sup>[86]</sup> Reproduced with permission from ref. [86]. Copyright (2017) Elsevier. b) Schematic of the O<sub>2</sub> crossover effect on pre-process Si anode in LIOBs.<sup>[88]</sup> Reproduced with permission from ref. [88]. Copyright (2016) The Royal Society of Chemistry. c) Oxygen crossover induced reactions occurring at the anode/electrolyte interphase of LIOBs in the OCV condition.<sup>[89]</sup> Reproduced with permission from ref. [89]. Copyright (2015) American Chemical Society.

metal-free LIOB realizes relatively high energy density based on the total electrode mass that is estimated as equal to 980 Wh kg<sup>-1</sup>. Similarly, a pre-lithiated Si anode that achieves a balance between reactive activity and specific capacity was matched with Ru/KB cathode, acquiring 100-cycle stable cycling with low potential hysteresis at 500 mA g<sup>-1</sup> and long-term operation under the protection of FEC-induced SEI (Figure 16b).<sup>[88]</sup> Furthermore, an inherently safe LIOB composed of nanostructured lithiated tin–carbon anode incorporating non-flammable ionic liquid-based electrolyte was proposed by Passerini, Hassoun and co-workers.<sup>[89]</sup> Nevertheless, oxygen crossover from cathode to anode followed by some parasitic reactions still deteriorates the battery performance (Figure 16c).

As a result of the hostless nature, Li–metal anode including the alloy above undergoes severe relative volume deformation during charge-discharge cycles which is another major obstacle to their application. From this perspective, constructing anode framework can not only reduce the current density by increasing the surface area and thus mitigate interfacial degeneration, but also accommodate the volume change of the electrode and hence greatly retain the stability of the SEI, which is beneficial to protect Li anode from erosion. For instance, a reduced graphene oxide (r-GO)/Li composite was prepared by the capillarity and lithophilic property of graphene oxide sheets to load molten Li.<sup>[90]</sup> The flexible r-GO matrix is able to stabilize the SEI and homogenize Li stripping/plating, therefore more uniform surface morphology was obtained on the r-GO/Li anode even under bending condition (Figure 17a). Recently, Ye et al.<sup>[91]</sup> reported a three-dimensional cross-stacked carbon nanotube network (3D-CSC) that possesses extremely light weight, large surface area and electrochemical stability (Figure 17b). After electro-depositing metallic Li, the 3D-CSC scaffold significantly enhanced the cycling performance of Li–O<sub>2</sub> batteries by inhibiting dendrite growth and stabilizing SEI.

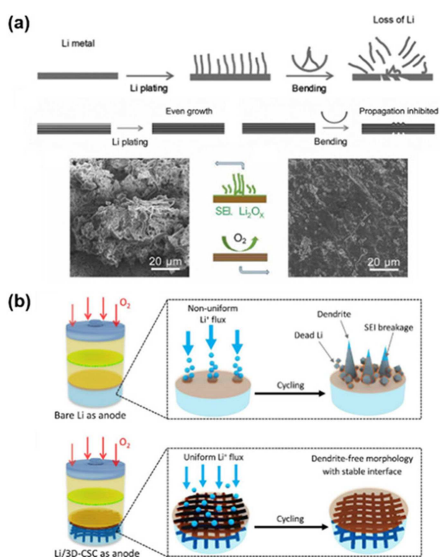


**Figure 17.** a) Surface morphology of the Li anode with or without r-GO modification under bending condition.<sup>[90]</sup> Reproduced with permission from ref. [90]. Copyright (2017) WILEY-VCH Verlag GmbH & Co. KGaA, Weinheim. b) Schematic diagram of the Li<sup>+</sup> deposition behavior on different Li-metal anode in Li–O<sub>2</sub> batteries.<sup>[91]</sup> Reproduced with permission from ref. [91]. Copyright (2019) WILEY-VCH Verlag GmbH & Co. KGaA, Weinheim.

Anode design plays an important role in stabilizing electrode structure, especially in maintaining the integrity of interphase. While oxygen, etc. crossover and moisture permeation yet aggravate the anodic interface resulting in electrode pulverization and consequent cell failure, particularly when the content of Li metal in anode is low. The rational interface design is also crucial for structured anode in Li–O<sub>2</sub> batteries.

## 5.2. Solid Electrolyte Interphase Improvement

As the critical component of battery R&D, SEI originates from interfacial chemistry and in turn affects interfacial reactions and Li deposition/dissolution behavior. By optimizing the composition and structure of SEI or constructing artificial SEI, some intractable issues such as abominable side reactions owing to the oxygen crossover and electrolyte reduction, dendritic Li deposition can be efficiently mitigated. On the whole, there are two main ways to improve SEI: one utilizing in-situ chemical or electrochemical reactions; the other by means of ex situ methods like doctor blading, dip-coating and so on. In-situ SEI has the characteristic of conformality so that it can realize remarkable protective effect with thin thickness. In addition, the simple fabrication method also makes it suitable for scalable manufacturing. In this regard, one effective and economic strategy is to use SEI forming additives in electrolyte, which preferentially react with Li-metal anode to generate durable SEI thereby avoiding electrolyte decomposition. Shen, Huang, and colleagues<sup>[39c]</sup> illustrated that the addition of boric acid (BA) in 1.0 M LiTFSI/DMSO could facilitate a continuous and dense SEI forming on the Li anode surface with the presence of oxygen. The storage test in humid air and

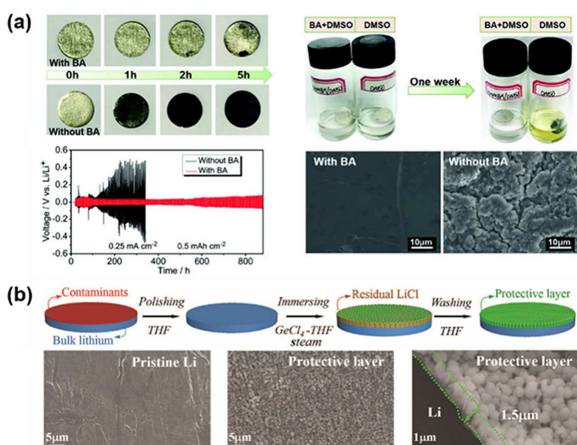


**Figure 18.** a) The stabilizing effect of boric acid additive on Li-metal anode.<sup>[39c]</sup> Reproduced with permission from ref. [39c]. Copyright (2018) WILEY-VCH Verlag GmbH & Co. KGaA, Weinheim. b) Modified procedures and SEM images of the protective layer on Li foils.<sup>[92]</sup> Reproduced with permission from ref. [92]. Copyright (2018) WILEY-VCH Verlag GmbH & Co. KGaA, Weinheim.

electrolyte demonstrated the superior barrier property against unwanted oxygen, moisture, electrolyte etc. (Figure 18a). Consequently, the cycle life of Li–O<sub>2</sub> cell with the BA additive extended more than six-fold. Apart from the operando reaction by employing additives, the in-situ SEI can also be constructed via pretreatment methods before battery assembly. As shown in Figure 18b,<sup>[92]</sup> the facile Li-metal preprocessing of soaking the Li metal in GeCl<sub>4</sub>-THF solution for several minutes was developed by Liao et al. Just five-minute treatment endows the germanium composite SEI with compact structure and appropriate thickness which exerts exceptionally protective effect on defense against water and dissolved oxygen attack.

Compared to the SEI obtained from in-situ chemical reaction, electrochemical process induced SEI is more tunable by controlling related parameters. In 2015, Zhang and co-workers<sup>[51d]</sup> reported a LiF-containing interfacial film, specifically several continuous charge-discharge cycles were operated in a Li||1 M LiF<sub>3</sub>SO<sub>3</sub> + TEGDME/FEC (5:1, v/v)||Li symmetric cell to construct the protection layer. Time dependence of the impedance spectra of the Li–O<sub>2</sub> battery with this modified anode display almost constant impedance change thanks to the protective effect of the electrochemical reaction induced SEI in terms of easing the Li anode corrosion by electrolyte and dissolved oxygen as it does inevitably increase the resistance and ultimately cause Li–O<sub>2</sub> battery failure (Figure 19a). Different from the additional electrochemical pretreatment device, directly electrochemical modification in a Li–O<sub>2</sub> full cell is a method of getting closer to actual operation. For instance, a homemade Li–CO<sub>2</sub> cell with the same configuration and composition as the Li–O<sub>2</sub> battery here expect for pure carbon dioxide atmosphere was presented by Asadi et al. to generate the Li<sub>2</sub>CO<sub>3</sub>/C coating for Li anode protection.<sup>[93]</sup> According to density functional theory (DFT) calculations, the elongated cycling lifetime from 11 cycles up to 700 cycles should be ascribed to the high migration energy barrier for oxygen and

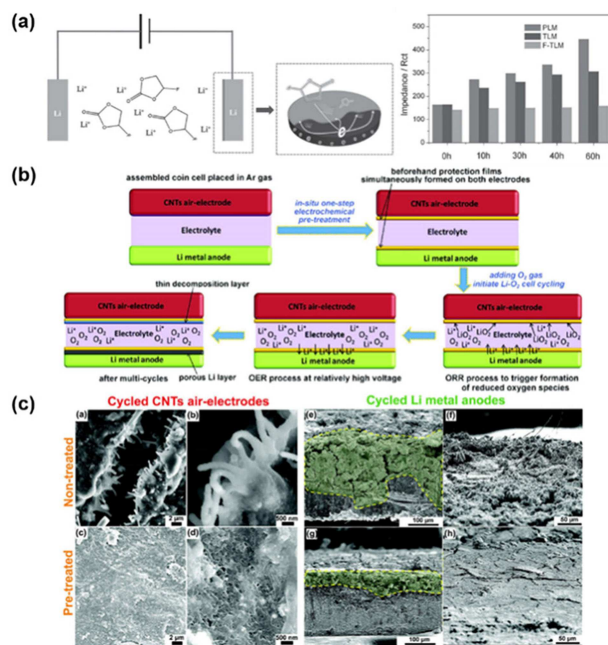


**Figure 19.** a) Scheme of the protective film forming on Li anode and impedance values change for the Li–O<sub>2</sub> cells with different anodes.<sup>[51d]</sup> Reproduced with permission from ref. [51d]. Copyright (2015) WILEY-VCH Verlag GmbH & Co. KGaA, Weinheim. b) Operation principle of the discharge/charge cycling of Li–O<sub>2</sub> battery obtained via in-situ one-step electrochemical process. c) SEM images of the non-treated and pre-treated CNTs air electrode and Li-metal anode.<sup>[23]</sup> Reproduced with permission from ref. [23]. Copyright (2018) WILEY-VCH Verlag GmbH & Co. KGaA, Weinheim.

nitrogen migrating through the  $\text{Li}_2\text{CO}_3$  layer. In other words, the  $\text{Li}_2\text{CO}_3/\text{C}$  coating has good barrier effect on preventing oxygen and nitrogen from contacting the Li anode and therefore improves the cycling capability. Similarly, Xu, Zhang, and colleagues<sup>[23]</sup> put forward a novel one-step electrochemical pre-charging strategy in argon environment prior to usual Li–O<sub>2</sub> battery charge/discharge cycle, which could form nanoscale thin films on the surface of both air cathode and Li-metal anode simultaneously (Figure 19b). Under the protection of in-situ SEI, thick bulk Li layer without corrosion and relatively flat surface layer with a few cracks were still preserved after 110 cycles in the Li–O<sub>2</sub> batteries (Figure 19c).

Another efficient approach of SEI promotion is to ex-situ synthesize artificial SEI. Because of the stronger operability, artificial SEI tends to be more robust than in-situ SEI that generally bonds so conformal with the Li substrate that it is hardly immune from the volume deformation of electrode. Additionally, uncontrollable compositional evolution, ultrathin thickness and other features also make in-situ SEI vulnerable to dendrite penetration and volume change upon cycling. As revealed in Figure 20a,<sup>[94]</sup> Sun and co-workers fabricated a stiff and uniform graphene-polydopamine composite layer (GPDL) on Li anode by drop-casting method. With the protective layer, Li–O<sub>2</sub> battery maintains over 150 cycles while delivering a high energy efficiency of 80% that achieve the objective of obtaining high-efficiency and long-lifetime Li–O<sub>2</sub> batteries thanks to the barrier property of GPDL in suppressing undesired reactions between Li anode with redox mediators as

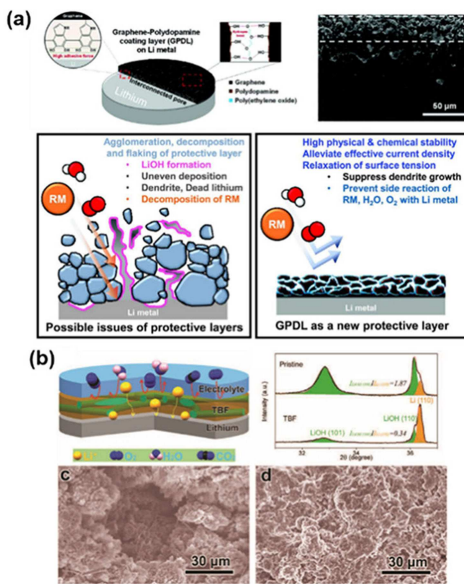


**Figure 20.** a) The schematic of the GPDL coating composition and efficacy.<sup>[94]</sup> Reproduced with permission from ref. [94]. Copyright (2017) WILEY-VCH Verlag GmbH & Co. KGaA, Weinheim. b) The protective effect of TBF on Li-metal anode during the cycling of Li–O<sub>2</sub> battery.<sup>[95]</sup> Reproduced with permission from ref. [95]. Copyright (2017) WILEY-VCH Verlag GmbH & Co. KGaA, Weinheim.

well as with oxygen and moisture. Considering the facile preparation procedures of solution-casting, Zhang's group<sup>[95]</sup> built an even stable lithiated Nafion-based composite layer on the surface of metallic Li with the help of familiar tissue. The X-ray diffraction analysis and SEM images illustrate the tissue-directed/reinforced bifunctional protection film (TBF) with outstanding mechanical and chemical stability significantly restrains the side reaction by separating Li metal from dissolved oxygen, moisture, and some discharge intermediates during the cycling (Figure 20b). As a result, improved reversibility and long lifetime are received in the Li–O<sub>2</sub> battery with the TBF-modified Li anode.

### 5.3. Barrier Layer Modification

Unlike the aforementioned general modification means, the indirect protection of Li-metal anode and even sustaining the stable operation of the entire battery by introducing a barrier layer has been widely investigated as a major distinction of the Li–O<sub>2</sub> cells from other seal-type Li metal batteries. Obviously, the barrier layers are established primarily to isolate undesirable components which give rise to serious side reactions. On the basis of various assembly positions of the barrier layer, the corresponding functional requirements are different. Among them, the barrier layer between the two electrodes mainly serves to protect the Li anode by blocking the diffusion of substances other than Li ions.<sup>[96]</sup> Lots of such protective layers and functional separators with water/oxygen impermeable features and suitable Li-ion conductivity are employed into Li–O<sub>2</sub> batteries. For example, Elia and Hassoun<sup>[97]</sup> casted a

PVDF-based gel polymer membrane with  $ZrO_2$  nanoparticles ceramic filler using a doctor blade. The insertion of the composite film between the anode and the separator mitigates the parasitic reaction caused by oxygen crossover, acquiring low interfacial impedance values and enhanced stability of the LIOB. Consideration of the high ionic conductivity and excellent mechanical property of the ceramic materials, a water-stable and water-impermeable Li-ion conducting solid electrolyte layer of  $Li_{1.3}Al_{0.5}Nb_{0.2}Ti_{1.3}(PO_4)_3$  (LTAP) was constructed by Shang and colleagues.<sup>[98]</sup> As shown in Figure 21a, the water

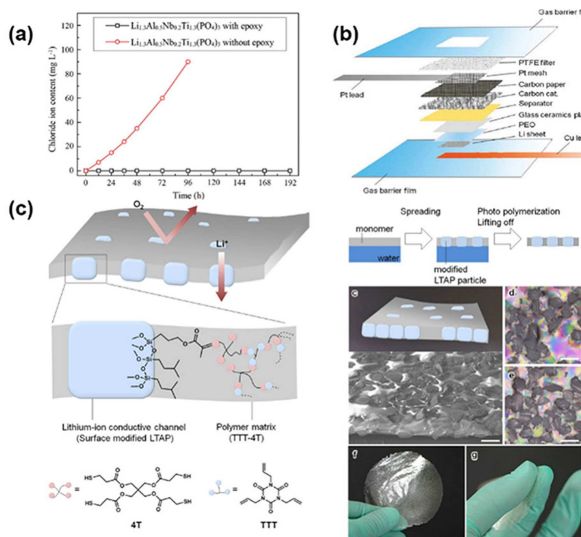


**Figure 21.** a) Water permeation test results for LANTP solid electrolyte layer with and without epoxy resin.<sup>[98]</sup> Reproduced with permission from ref. [98]. Copyright (2018) Elsevier. b) Schematic of the Li–O<sub>2</sub> battery with PEO buffer layer and LATP glass-ceramic electrolyte layer.<sup>[99]</sup> Reproduced with permission from ref. [99]. Copyright (2010) The Royal Society of Chemistry. c) The composition, preparation, structure, and morphology of the composite membrane.<sup>[100]</sup> Reproduced with permission from ref. [100]. Copyright (2017) Springer Nature.

permeation tests indicate the LANTP layer can efficiently prevent moisture from infiltrating with epoxy resin filled in open pores. The aqueous Li–O<sub>2</sub> battery with this ceramic layer exhibited a specific energy density of 984 Wh kg<sup>-1</sup> calculated based on the mass of anode, water, oxygen and MnO<sub>2</sub> at a current density of 0.32 mA cm<sup>-2</sup>. Integrating their respective advantages of organic and inorganic barriers, Imanishi and co-workers<sup>[99]</sup> proposed a rechargeable Li–O<sub>2</sub> battery conformation combining the acetic acid and water stable LATP glass-ceramic electrolyte layer with the Li metal-stable polyethylene oxide (PEO) buffer layer (Figure 21b). Besides, more novel is the elaborate design of the barrier layer. Choi et al.<sup>[100]</sup> demonstrated a new composite membrane composed of polymer matrix with surface-modified LATP particles throughout it via improved float-casting method (Figure 21c). The tight bonding between the matrix component and the surface modification layer on the glass-ceramic particles endows good air-tight characteristic to the ion-channel aligned membrane. Compared with the commonly thick ceramic layer, this composite membrane overcomes the weakness of high specific gravity

and fragility without compromising ionic conductivity and gas-blocking property.

It is also a facile way to construct the barrier layer by directly modifying the separator without introducing other intercalations. Choi and co-workers<sup>[101]</sup> designed a non-porous polyurethane (PU) separator with excellent air impermeability because of the high chain packing densities. The presence of hard and soft segments endows PU separator with mechanical strength as well as flexibility (Figure 22a). Therefore, the cycle

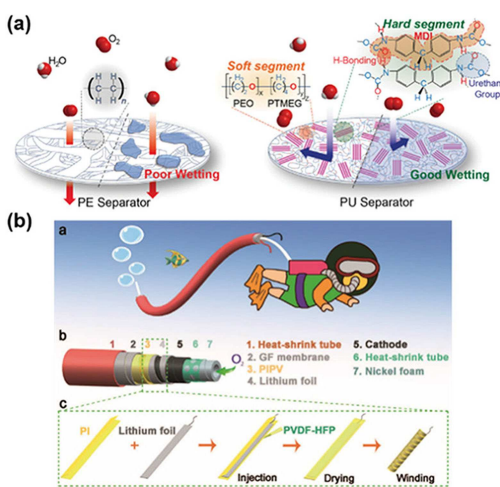


**Figure 22.** a) Schematic representation for the effect of composition and structure on the PU separator property.<sup>[101]</sup> Reproduced with permission from ref. [101]. Copyright (2016) WILEY-VCH Verlag GmbH & Co. KGaA, Weinheim. b) Schematic illustration on the possible practical application, architecture, and preparation of the PIPV membrane in safe flexible Li–O<sub>2</sub> battery.<sup>[102]</sup> Reproduced with permission from ref. [102]. Copyright (2017) WILEY-VCH Verlag GmbH & Co. KGaA, Weinheim.

life of the Li–O<sub>2</sub> battery with the PU film increases to 110 cycles comparing with 56 cycles of the porous polyethylene separator at a current density of 200 mA g<sup>-1</sup>. In another research, a flexible polyimide and poly (vinylidene fluoride-co-hexafluoropropylene) composite (PIPV) separator was fabricated by Yin et al.<sup>[102]</sup> As illustrated in Figure 22b, the PIPV membrane possesses superb waterproof property and hence Li–O<sub>2</sub> battery with the creative architecture delivers superior cycling stability over 200 cycles at a current of 1 mA and capacity of 4 mAh.

There is another barrier layer that is attached to the outer side of the air-cathode or covers the whole cell as the packaging material. For such barrier layer, it needs to prevent the invasion of all substances except oxygen, that is to say, this barrier layer functions more as the oxygen selective membrane (OSM) to keep the operation of Li–O<sub>2</sub> battery.<sup>[96]</sup> Peng and colleagues<sup>[103]</sup> developed a low-density polyethylene (LDPE) film outside the carbon nanotube air electrode to block water permeation which could accelerate the irreversible transformation of the discharge product to Li<sub>2</sub>CO<sub>3</sub> (Figure 23a). The non-polar molecular structure of the LDPE membrane plays an important role in infiltrating oxygen selectively. With the LDPE membrane, the discharge voltage of Li–O<sub>2</sub> battery maintains over 325 cycles without any distinct change at a current density

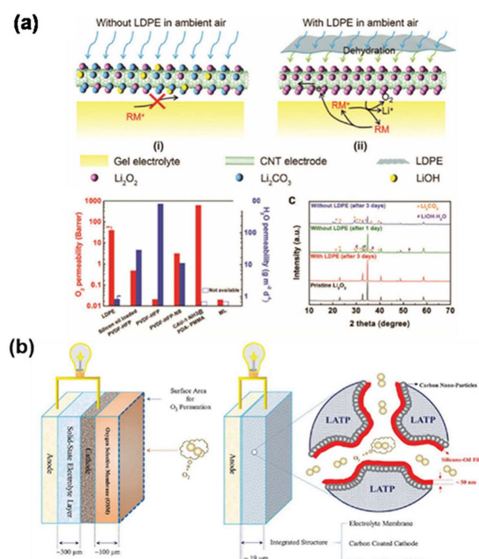


**Figure 23.** a) Critical role of the LDPE film in Li–O<sub>2</sub> battery.<sup>[103]</sup> Reproduced with permission from ref. [103]. Copyright (2017) WILEY-VCH Verlag GmbH & Co. KGaA, Weinheim. b) Schematic illustration to the different architectures of solid-state Li–air batteries.<sup>[105]</sup> Reproduced with permission from ref. [105]. Copyright (2015) The Royal Society of Chemistry.

of 2000 mA g<sup>-1</sup> in ambient air (~50% relative humidity). The oxygen selective membrane can also be readily synthesized from silicone oil in which oxygen has a higher solubility and diffusivity than water. In 2010, Zhang et al.<sup>[104]</sup> reported the silicone oil film not only impedes the ingress of moisture from air, but also retards liquid electrolyte evaporation, which enables a non-aqueous Li–O<sub>2</sub> battery with the OSM to discharge in ambient atmosphere (20% relative humidity) for 16.3 days with a specific capacity of 789 mA h g<sub>carbon</sub><sup>-1</sup> at a current density of 0.05 mA cm<sup>-2</sup>. Subsequently, Zhao and co-workers<sup>[105]</sup> applied the silicone oil to a solid-state Li–air battery where the solid electrolyte and the air-cathode skeleton were fabricated using the same material (LATP) but had different compactness (Figure 23b). About 50 nm-thick silicone oil membrane that was prepared via an infiltration process covers on the carbon-coated LATP surface with highly expended area as the OSM to obstruct moisture and carbon dioxide. Consequently, the solid-state Li–O<sub>2</sub> cell with this OSM remains steady cycling for 50 cycles in ambient air (~50% relative humidity) with the fixed capacity of 5000 mA h g<sub>carbon</sub><sup>-1</sup> at a current density of 0.3 mA cm<sup>-2</sup>.

## 6. Conclusion and Perspectives

In summary, practical Li-metal anode confronts two severe challenges, Li dendrite and unstable SEI formation, which practically lead to low coulombic efficiency and even short circuit. Systematical characterizations of dendrite growth and SEI evolution are therefore of great significance to reveal the fundamental mechanism and raise modification methods accordingly, which are summarized and categorized in this review. It is worth noting that each characterization technique

has its own advantages and limitations due to specific operating principles. For example, microscopic techniques (e.g. SEM, TEM, AFM, etc.) can visualize microstructure down to atomic-scale resolution, yet are limited to local areas probe. Spectroscopic techniques (e.g. XPS, FTIR, Raman, NMR, XAS, etc.) are particularly sensitive to chemical shift, functional groups, molecular structure or electronic structure, but the probing depth is usually thin. As a result, the comparison and combination of diverse techniques are essential to obtain an in-depth and comprehensive understanding on Li-metal anode related scientific issues.

Up to now, plentiful investigations have been reported on Li dendrite growth and SEI composition by diverse characterization techniques, however, this challenging research field still needs introducing other advanced characterization techniques or even develop novel characterization methodology. Note that both Li dendrite and SEI are highly active in interfacial scale, inappropriate operation may happen when we disassemble the battery, separate the electrode, wash the electrode with organic solvents and remove the sample to be tested etc. Hence, the ultrafine surface morphology, detailed composition and microstructure may not be well maintained. Imperceptible reactions between electrode and environment may further decrease the reliability of achieved data. Cryo-microscopy is a promising technique which can well preserve the original states as much as possible. Although there has been no report on Li–O<sub>2</sub> batteries with cryo-microscopy, this technique itself has demonstrated advantages in investigating Li metal related topics. Meanwhile, in-situ and operando characterization is another strategy to get convincing results with time resolution, but the experimental set up still need careful design in the further works on Li–O<sub>2</sub> batteries.

In addition to universal challenges such as Li dendrite, ultrahigh activity and large volume change faced by Li metal, there are three particular significant differences for Li metal in Li–O<sub>2</sub> batteries compared with other type Li metal batteries such as Li-sulfur batteries: (i) The cathode of Li–O<sub>2</sub> batteries is an open or semi-open system which means that the anode corrosion caused by some contamination such as oxygen and moisture diffused from cathode side is a huge and inevitable challenge; (ii) Ether electrolyte is usually used in Li–O<sub>2</sub> batteries instead of ester type due to its severe side reactions with intermediate product Li<sub>2</sub>O and Li metal, which leads to a narrow electrochemical window meanwhile the side reactions still exist; (iii) The redox mediators such as LiI can also react with Li metal and cause corrosion. As for the special corrosion challenge, effective and common solutions refer to alloying, in-situ SEI and ex-situ SEI which are suitable for other types of Li metal batteries. As for electrochemical window, the promising strategy is to utilize solid state electrolyte which can not only alleviate side reactions and widen the electrochemical window but also inhibit Li dendrite. With the development of parallel battery technology, solid state Li–O<sub>2</sub> batteries based on Li ion conducting inorganic ceramics or organic polymers were thought to be promising candidates and have aroused widespread research interest. By replacing the volatile and flammable organic solvent, solid state Li–O<sub>2</sub> batteries possesses

considerable advantages including superior safety, improved resistance against desiccation, wider operation temperature range, longer service life and lower cost. While the low ionic conductivities of prevailing solid electrolyte and the extremely large internal resistance across solid-solid contact is major obstacle to the development solid state batteries. Due to the peculiar operation principles, Li–O<sub>2</sub> batteries further suffer from issues such as oxygen transport, reaction product accumulation and stability against oxygen reduction species. These features have brought about extra difficulties to the experimental preparation, characterization and analysis of Li anode behavior during battery operation, where both opportunities and challenges lie ahead.

Despite the daunting challenges in developing practical accessible Li–O<sub>2</sub> batteries, researchers have paved way forward and made considerable progresses so far. Based on previous characterization results, various and effective modification techniques for Li-metal anode have been proposed. On the one hand, alloying and structure design together with solid state electrolyte are three main modification methods to suppress Li dendrite. On the other hand, in-situ and ex-situ SEI as well as electrolyte additives are usually reported to contribute to a stable SEI. Various additives are quite interesting and meaningful. However, it should be noticed that Li–O<sub>2</sub> batteries performance is not simply determined by the Li anode, but also affected by cathode and electrolyte. In the case of solid-state Li–O<sub>2</sub> batteries, the interface between cathode and solid electrolyte further need to be considered to optimize overall battery performance. As a result, the comprehensive, systematic and integrated characterizations on cathode, anode, electrolyte and interfaces are prerequisites to the practical development of Li–O<sub>2</sub> batteries, which calls for worldwide investigations and cooperation.

All in all, the review carried out a series of discussions from fundamental chemistry to advanced characterization techniques and effective modification methods towards safe Li-metal anode of Li–O<sub>2</sub> batteries. Tough as it may be, high-performance Li–O<sub>2</sub> batteries will be realized with the gradually increased understanding of their in-depth mechanisms by more and more advanced characterization techniques together with effective modifications.

## Acknowledgements

This work was supported by National Key Research and Development Program (2016YFA0202500), National Natural Science Foundation of China (51822211, 21776019, 21676160 and 21825501), Beijing Municipal Science & Technology Commission (Grants No. D181100004518003), and Beijing Key Research and Development Plan (Z181100004518001).

## Conflict of Interest

The authors declare no conflict of interest.

**Keywords:** Li–O<sub>2</sub> batteries · lithium metal anode · advanced characterization · effective modifications

- [1] D. Aurbach, B. D. McCloskey, L. F. Nazar, P. G. Bruce, *Nat. Energy* **2016**, *1*, 16128.
- [2] A. C. Luntz, B. D. McCloskey, *Chem. Rev.* **2014**, *114*, 11721–11750.
- [3] L. Ma, T. Yu, E. Tzoganakis, K. Amine, T. Wu, Z. Chen, J. Lu, *Adv. Energy Mater.* **2018**, *8*, 1800348.
- [4] a) J.-S. Lee, S. Tai Kim, R. Cao, N.-S. Choi, M. Liu, K. T. Lee, J. Cho, *Adv. Energy Mater.* **2011**, *1*, 34–50; b) Y. Li, J. Lu, *ACS Energy Lett.* **2017**, *2*, 1370–1377.
- [5] Z. Lyu, Y. Zhou, W. Dai, X. Cui, M. Lai, L. Wang, F. Huo, W. Huang, Z. Hu, W. Chen, *Chem. Soc. Rev.* **2017**, *46*, 6046–6072.
- [6] N. Imanishi, O. Yamamoto, *Mater. Today* **2014**, *17*, 24–30.
- [7] a) N. Feng, P. He, H. Zhou, *Adv. Energy Mater.* **2016**, *6*, 1502303; b) J. Christensen, P. Albertus, R. S. Sanchez-Carrera, T. Lohmann, B. Kozinsky, R. Liedtke, J. Ahmed, A. Kojic, *J. Electrochem. Soc.* **2011**, *159*, R1–R30.
- [8] Y. Wang, H. Zhou, *J. Power Sources* **2010**, *195*, 358–361.
- [9] X.-B. Cheng, C.-Z. Zhao, Y.-X. Yao, H. Liu, Q. Zhang, *Chem* **2019**, *5*, 74–96.
- [10] Y. Sun, *Nano Energy* **2013**, *2*, 801–816.
- [11] D. Geng, N. Ding, T. S. A. Hor, S. W. Chien, Z. Liu, D. Wuu, X. Sun, Y. Zong, *Adv. Energy Mater.* **2016**, *6*, 1502164.
- [12] P. G. Bruce, S. A. Freunberger, L. J. Hardwick, J. M. Tarascon, *Nat. Mater.* **2011**, *11*, 19–29.
- [13] G. Girishkumar, B. McCloskey, A. C. Luntz, S. Swanson, W. Wilcke, *J. Phys. Chem. Lett.* **2010**, *1*, 2193–2203.
- [14] a) X.-B. Cheng, R. Zhang, C.-Z. Zhao, Q. Zhang, *Chem. Rev.* **2017**, *117*, 10403–10473; b) X.-Q. Zhang, C.-Z. Zhao, J.-Q. Huang, Q. Zhang, *Engineering* **2018**, *4*, 831–847.
- [15] a) Z. Huang, J. Ren, W. Zhang, M. Xie, Y. Li, D. Sun, Y. Shen, Y. Huang, *Adv. Mater.* **2018**, *30*, 1803270; b) X. Lei, X. Liu, W. Ma, Z. Cao, Y. Wang, Y. Ding, *Angew. Chem. Int. Ed.* **2018**, *57*, 16131–16135.
- [16] J. B. Park, S. H. Lee, H. G. Jung, D. Aurbach, Y. K. Sun, *Adv. Mater.* **2018**, *30*, 1704162.
- [17] a) B. G. Kim, J.-S. Kim, J. Min, Y.-H. Lee, J. H. Choi, M. C. Jang, S. A. Freunberger, J. W. Choi, *Adv. Funct. Mater.* **2016**, *26*, 1747–1756; b) T. Zhang, H. Matsuda, H. Zhou, *ChemSusChem* **2014**, *7*, 2845–2852; c) J. Lu, Y. Lei, K. C. Lau, X. Luo, P. Du, J. Wen, R. S. Assary, U. Das, D. J. Miller, J. W. Elam, H. M. Albishri, D. A. El-Hady, Y.-K. Sun, L. A. Curtiss, K. Amine, *Nat. Commun.* **2013**, *4*, 2383.
- [18] M. Asadi, B. Sayahpour, P. Abbasi, A. T. Ngo, K. Karis, J. R. Jokisaari, C. Liu, B. Narayanan, M. Gerard, P. Yasaei, X. Hu, A. Mukherjee, K. C. Lau, R. S. Assary, F. Khalili-Araghi, R. F. Klie, L. A. Curtiss, A. Salehi-Khojin, *Nature* **2018**, *555*, 502–506.
- [19] a) J. Hassoun, H. G. Jung, D. J. Lee, J. B. Park, K. Amine, Y. K. Sun, B. Scrosati, *Nano Lett.* **2012**, *12*, 5775–5779; b) S. A. Freunberger, Y. Chen, Z. Peng, J. M. Griffin, L. J. Hardwick, F. Barde, P. Novak, P. G. Bruce, *J. Am. Chem. Soc.* **2011**, *133*, 8040–8047; c) S. A. Freunberger, Y. Chen, N. E. Drewett, L. J. Hardwick, F. Bardé, P. G. Bruce, *Angew. Chem. Int. Ed.* **2011**, *50*, 8609–8613; *Angew. Chem.* **2011**, *123*, 8768–8772.
- [20] a) S. Wu, K. Zhu, J. Tang, K. Liao, S. Bai, J. Yi, Y. Yamauchi, M. Ishida, H. Zhou, *Energy Environ. Sci.* **2016**, *9*, 3262–3271; b) R. Younesi, G. M. Veith, P. Johansson, K. Edström, T. Vegge, *Energy Environ. Sci.* **2015**, *8*, 1905–1922.
- [21] a) D. Lin, Y. Liu, Y. Cui, *Nat. Nanotechnol.* **2017**, *12*, 194–206; b) X. Q. Zhang, X. B. Cheng, Q. Zhang, *Adv. Mater. Interfaces* **2018**, *5*, 1701097; c) W. Xu, J. Wang, F. Ding, X. Chen, E. Nasibulin, Y. Zhang, J.-G. Zhang, *Energy Environ. Sci.* **2014**, *7*, 513–537; d) X.-B. Cheng, C.-Z. Zhao, Y.-X. Yao, H. Liu, Q. Zhang, *Chem* **2019**, *5*, 74–96; e) H. Kim, G. Jeong, Y. U. Kim, J. H. Kim, C. M. Park, H. J. Sohn, *Chem. Soc. Rev.* **2013**, *42*, 9011–9034; f) A. C. Luntz, B. D. McCloskey, *Chem. Rev.* **2014**, *114*, 11721–11750; g) K. Zhang, G.-H. Lee, M. Park, W. Li, Y.-M. Kang, *Adv. Energy Mater.* **2016**, *6*, 1600811; h) K. N. Wood, M. Noked, N. P. Dasgupta, *ACS Energy Lett.* **2017**, *2*, 664–672.
- [22] P. Verma, P. Maire, P. Novák, *Electrochim. Acta* **2010**, *55*, 6332–6341.
- [23] B. Liu, W. Xu, J. Tao, P. Yan, J. Zheng, M. H. Engelhard, D. Lu, C. Wang, J.-G. Zhang, *Adv. Energy Mater.* **2018**, *8*, 1702340.
- [24] X. Wang, M. Zhang, J. Alvarado, S. Wang, M. Sina, B. Lu, J. Bouwer, W. Xu, J. Xiao, J. G. Zhang, J. Liu, Y. S. Meng, *ACS Energy Lett.* **2017**, *17*, 7606–7612.

- [25] A. J. Leenheer, K. L. Jungjohann, K. R. Zavadil, J. P. Sullivan, C. T. Harris, *ACS Nano* **2015**, *9*, 4379–4389.
- [26] J. L. Shui, J. S. Okasinski, P. Kenesei, H. A. Dobbs, D. Zhao, J. D. Almer, D. J. Liu, *Nat. Commun.* **2013**, *4*, 2255.
- [27] J. Steiger, D. Kramer, R. Möning, *J. Power Sources* **2014**, *261*, 112–119.
- [28] a) H. Sano, H. Sakaebe, H. Matsumoto, *J. Power Sources* **2011**, *196*, 6663–6669; b) W. Li, H. Yao, K. Yan, G. Zheng, Z. Liang, Y. M. Chiang, Y. Cui, *Nat. Commun.* **2015**, *6*, 7436; c) J. Wang, J. Liu, Y. Cai, F. Cheng, Z. Niu, J. Chen, *ChemElectroChem* **2018**, *5*, 1702–1707.
- [29] L. Suo, Y. S. Hu, H. Li, M. Armand, L. Chen, *Nat. Commun.* **2013**, *4*, 1481.
- [30] L. Ye, M. Liao, H. Sun, Y. Yang, C. Tang, Y. Zhao, L. Wang, Y. Xu, L. Zhang, B. Wang, F. Xu, X. Sun, Y. Zhang, H. Dai, P. G. Bruce, H. Peng, *Angew. Chem. Int. Ed.* **2019**, *58*, 1–7.
- [31] M. Golozar, P. Hovington, A. Paolella, S. Bessette, M. Lagace, P. Bouchard, H. Demers, R. Gauvin, K. Zaghib, *Nano Lett.* **2018**, *18*, 7583–7589.
- [32] H. Zheng, D. Xiao, X. Li, Y. Liu, Y. Wu, J. Wang, K. Jiang, C. Chen, L. Gu, X. Wei, Y. S. Hu, Q. Chen, H. Li, *Nano Lett.* **2014**, *14*, 4245–4249.
- [33] G. Zheng, S. W. Lee, Z. Liang, H. W. Lee, K. Yan, H. Yao, H. Wang, W. Li, S. Chu, Y. Cui, *Nat. Nanotechnol.* **2014**, *9*, 618–623.
- [34] R. L. Sacci, J. M. Black, N. Balke, N. J. Dudney, K. L. More, R. R. Unocic, *Nano Lett.* **2015**, *15*, 2011–2018.
- [35] a) K.-i. Morigaki, A. Ohta, *J. Power Sources* **1998**, *76*, 159–166; b) D. Aurbach, B. Markovsky, M. D. Levi, E. Levi, A. Schechter, M. Moshkovich, Y. Cohen, *J. Power Sources* **1999**, *81*–*82*, 95–111; c) Y. S. Cohen, Y. Cohen, D. Aurbach, *J. Phys. Chem. B* **2000**, *104*, 12282–12291; d) N. W. Li, Y. X. Yin, C. P. Yang, Y. G. Guo, *Adv. Mater.* **2016**, *28*, 1853–1858.
- [36] K. J. Harry, D. T. Hallinan, D. Y. Parkinson, A. A. MacDowell, N. P. Balsara, *Nat. Mater.* **2014**, *13*, 69–73.
- [37] F. Sun, R. Gao, D. Zhou, M. Osenberg, K. Dong, N. Kardjilov, A. Hilger, H. Markötter, P. M. Bieker, X. Liu, I. Manke, *ACS Energy Lett.* **2018**, *4*, 306–316.
- [38] R. S. Assary, J. Lu, P. Du, X. Luo, X. Zhang, Y. Ren, L. A. Curtiss, K. Amine, *ChemSusChem* **2013**, *6*, 51–55.
- [39] a) C. K. Lee, Y. J. Park, *ACS Appl. Mater. Interfaces* **2016**, *8*, 8561–8567; b) V. S. Bryantsev, V. Giordani, W. Walker, J. Uddin, I. Lee, A. C. T. van Duin, G. V. Chase, D. Addison, *J. Phys. Chem. C* **2013**, *117*, 11977–11988; c) Z. Huang, J. Ren, W. Zhang, M. Xie, Y. Li, D. Sun, Y. Shen, Y. Huang, *Adv. Mater.* **2018**, *30*, e1803270; d) X. Zou, Q. Lu, Y. Zhong, K. Liao, W. Zhou, Z. Shao, *Small* **2018**, *14*, e1801798; e) Y. Kim, D. Koo, S. Ha, S. C. Jung, T. Yim, H. Kim, S. K. Oh, D. M. Kim, A. Choi, Y. Kang, K. H. Ryu, M. Jang, Y. K. Han, S. M. Oh, K. T. Lee, *ACS Nano* **2018**, *12*, 4419–4430; f) X. Zhang, Q. Zhang, X. G. Wang, C. Wang, Y. N. Chen, Z. Xie, Z. Zhou, *Angew. Chem. Int. Ed.* **2018**, *57*, 12814–12818; g) D. J. Lee, H. Lee, J. Song, M.-H. Ryou, Y. M. Lee, H.-T. Kim, J.-K. Park, *Electrochim. Commun.* **2014**, *40*, 45–48.
- [40] Z. Moghadam, M. Shabani-Nooshabadi, M. Behpour, *J. Molecular Liquids* **2017**, *242*, 971–978.
- [41] a) Y. Chen, S. A. Freunberger, Z. Peng, O. Fontaine, P. G. Bruce, *Nat. Chem.* **2013**, *5*, 489–494; b) K. Pranay Reddy, P. Fischer, M. Marinaro, M. Wohlfahrt-Mehrens, *ChemElectroChem* **2018**, *5*, 2758–2766; c) F. Marchioni, K. Star, E. Menke, T. Buffeteau, L. Servant, B. Dunn, F. Wudl, *Langmuir* **2007**, *23*, 11597–11602; d) C. Naudin, J. L. Bruneel, M. Chami, B. Desbat, J. Grondin, J. C. Lassègues, L. Servant, *J. Power Sources* **2003**, *124*, 518–525.
- [42] a) K.-i. Morigaki, *J. Power Sources* **2002**, *104*, 13–23; b) K. Kanamura, *J. Electrochem. Soc.* **1997**, *144*, 1900.
- [43] a) F. S. Gittleson, K. P. C. Yao, D. G. Kwabi, S. Y. Sayed, W.-H. Ryu, Y. Shao-Horn, A. D. Taylor, *ChemElectroChem* **2015**, *2*, 1446–1457; b) W. Dai, X. Cui, Y. Zhou, Y. Zhao, L. Wang, L. Peng, W. Chen, *Small Methods* **2018**, 1800358.
- [44] a) I. Rey, *J. Electrochem. Soc.* **1998**, *145*, 3034; b) I. Rey, J. C. Lassègues, P. Baudry, H. Majastre, *Electrochim. Acta* **1998**, *43*, 1539–1544.
- [45] J. L. Bruneel, J. C. Lassègues, C. Sourisseau, *J. Raman Spectrosc.* **2002**, *33*, 815–828.
- [46] G. Li, H. Li, Y. Mo, L. Chen, X. Huang, *J. Power Sources* **2002**, *104*, 190–194.
- [47] T. A. Galloway, L. Cabo-Fernandez, I. M. Aldous, F. Braga, L. J. Hardwick, *Faraday Discuss.* **2017**, *205*, 469–490.
- [48] R. Bhattacharyya, B. Key, H. Chen, A. S. Best, A. F. Hollenkamp, C. P. Grey, *Nat. Mater.* **2010**, *9*, 504–510.
- [49] G. Nazri, *J. Electrochem. Soc.* **1985**, *132*, 2050.
- [50] C. Fiedler, B. Luerssen, M. Rohnke, J. Sann, J. Janek, *J. Electrochem. Soc.* **2017**, *164*, A3742–A3749.
- [51] a) J. Qian, W. A. Henderson, W. Xu, P. Bhattacharya, M. Engelhard, O. Borodin, J. G. Zhang, *Nat. Commun.* **2015**, *6*, 6362; b) Y. Lu, Z. Tu, L. A. Archer, *Nat. Mater.* **2014**, *13*, 961–969; c) B. G. Kim, J.-S. Kim, J. Min, Y.-H. Lee, J. H. Choi, M. C. Jang, S. A. Freunberger, J. W. Choi, *Adv. Funct. Mater.* **2016**, *26*, 1747–1756; d) Q. C. Liu, J. J. Xu, S. Yuan, Z. W. Chang, D. Xu, Y. B. Yin, L. Li, H. X. Zhong, Y. S. Jiang, J. M. Yan, X. B. Zhang, *Adv. Mater.* **2015**, *27*, 5241–5247.
- [52] a) C. Li, J. Wei, P. Li, W. Tang, W. Feng, J. Liu, Y. Wang, Y. Xia, *Sci. Bull.* **2019**; b) J. Zhang, B. Sun, Y. Zhao, A. Tkacheva, Z. Liu, K. Yan, X. Guo, A. M. McDonagh, D. Shanmukaraj, C. Wang, T. Rojo, M. Armand, Z. Peng, G. Wang, *Nat. Commun.* **2019**, *10*, 602; c) Y. Yu, Y.-B. Yin, J.-L. Ma, Z.-W. Chang, T. Sun, Y.-H. Zhu, X.-Y. Yang, T. Liu, X.-B. Zhang, *Energy Storage Mater.* **2019**, *18*, 382–388.
- [53] a) Z. Zeng, W. I. Liang, H. G. Liao, H. L. Xin, Y. H. Chu, H. Zheng, *Nano Lett.* **2014**, *14*, 1745–1750; b) H.-W. Lee, Y. Li, Y. Cui, *Current Opinion Chem. Eng.* **2016**, *12*, 37–43.
- [54] a) J. Lu, Y. Lei, K. C. Lau, X. Luo, P. Du, J. Wen, R. S. Assary, U. Das, D. J. Miller, J. W. Elam, H. M. Albishri, D. A. El-Hady, Y. K. Sun, L. A. Curtiss, K. Amine, *Nat. Commun.* **2013**, *4*, 2383; b) H. G. Jung, H. S. Kim, J. B. Park, I. H. Oh, J. Hassoun, C. S. Yoon, B. Scrosati, Y. K. Sun, *Nano Lett.* **2012**, *12*, 4333–4335.
- [55] R. R. Unocic, X. G. Sun, R. L. Sacci, L. A. Adamczyk, D. H. Alsem, S. Dai, N. J. Dudney, K. L. More, *Microsc. Microanal.* **2014**, *20*, 1029–1037.
- [56] R. L. Sacci, N. J. Dudney, K. L. More, L. R. Parent, I. Arslan, N. D. Browning, R. R. Unocic, *Chem. Commun.* **2014**, *50*, 2104–2107.
- [57] M. J. Zachman, Z. Tu, S. Choudhury, L. A. Archer, L. F. Kourkoutis, *Nature* **2018**, *560*, 345–349.
- [58] B. Liu, W. Xu, J. Tao, P. Yan, J. Zheng, M. H. Engelhard, D. Lu, C. Wang, J.-G. Zhang, *Adv. Energy Mater.* **2018**, *8*, 1702340.
- [59] K. Dong, H. Markotter, F. Sun, A. Hilger, N. Kardjilov, J. Banhart, I. Manke, *ChemSusChem* **2019**, *12*, 261–269.
- [60] K. Nishikawa, T. Mori, T. Nishida, Y. Fukunaka, M. Rosso, T. Homma, *J. Electrochem. Soc.* **2010**, *157*, A1212.
- [61] J. Wandt, C. Marino, H. A. Gasteiger, P. Jakes, R.-A. Eichel, J. Granwehr, *Energy Environ. Sci.* **2015**, *8*, 1358–1367.
- [62] S. Chandrashekhar, N. M. Trease, H. J. Chang, L. S. Du, C. P. Grey, A. Jerschow, *Nat. Mater.* **2012**, *11*, 311–315.
- [63] R. E. Gerald, C. S. Johnson, J. W. Rathke, R. J. Klingler, G. Sandí, L. G. Scanlon, *J. Power Sources* **2000**, *89*, 237–243.
- [64] S. Ganapathy, B. D. Adams, G. Stenou, M. S. Anastasaki, K. Goubitz, X. F. Miao, L. F. Nazar, M. Wagemaker, *J. Am. Chem. Soc.* **2014**, *136*, 16335–16344.
- [65] S. Walus, C. Barchasz, J. F. Colin, J. F. Martin, E. Elkaim, J. C. Lepretre, F. Alloin, *Chem. Commun.* **2013**, *49*, 7899–7901.
- [66] J. Lu, Y. J. Lee, X. Luo, K. C. Lau, M. Asadi, H. H. Wang, S. Brombosz, J. Wen, D. Zhai, Z. Chen, D. J. Miller, Y. S. Jeong, J. B. Park, Z. Z. Fang, B. Kumar, A. Salehi-Khojin, Y. K. Sun, L. A. Curtiss, K. Amine *Nature* **2016**, *529*(7586), 377–382.
- [67] A. Schechter, D. Aurbach, H. Cohen, *Langmuir* **1999**, *15*, 3334–3342.
- [68] a) F. Ding, W. Xu, G. L. Graff, J. Zhang, M. L. Sushko, X. Chen, Y. Shao, M. H. Engelhard, Z. Nie, J. Xiao, X. Liu, P. V. Sushko, J. Liu, J. G. Zhang, *J. Am. Chem. Soc.* **2013**, *135*, 4450–4456; b) Z. Huang, J. Ren, W. Zhang, M. Xie, Y. Li, D. Sun, Y. Shen, Y. Huang, *Adv. Mater.* **2018**, *30*, e1803270.
- [69] D. Aurbach, *J. Electrochem. Soc.* **1987**, *134*, 1611.
- [70] F. S. Gittleson, W. H. Ryu, A. D. Taylor, *ACS Appl. Mater. Interfaces* **2014**, *6*, 19017–19025.
- [71] a) G. S. Hutchings, J. Rosen, D. Smiley, G. R. Goward, P. G. Bruce, F. Jiao, *J. Phys. Chem. C* **2014**, *118*, 12617–12624; b) B. M. Gallant, D. G. Kwabi, R. R. Mitchell, J. Zhou, C. V. Thompson, Y. Shao-Horn, *Energy Environ. Sci.* **2013**, *6*, 2518.
- [72] L. Y. Lim, S. Fan, H. H. Hng, M. F. Toney, *Adv. Energy Mater.* **2015**, *5*, 1500599.
- [73] a) M. Letellier, F. Chevallier, M. Morcrette, *Carbon* **2007**, *45*, 1025–1034; b) B. Key, R. Bhattacharyya, M. Morcrette, V. Seznec, J. M. Tarascon, C. P. Grey, *J. Am. Chem. Soc.* **2009**, *131*, 9239–9249.
- [74] L. A. Huff, J. L. Rapp, L. Zhu, A. A. Gewirth, *J. Power Sources* **2013**, *235*, 87–94.
- [75] T. Liu, Z. Liu, G. Kim, J. T. Frith, N. Garcia-Araez, C. P. Grey, *Angew. Chem. Int. Ed.* **2017**, *56*, 16057–16062; *Angew. Chem.* **2017**, *129*, 16273–16278.
- [76] M. Leskes, A. J. Moore, G. R. Goward, C. P. Grey, *J. Phys. Chem. C* **2013**, *117*, 26929–26939.

- [77] H. G. Jung, J. Hassoun, J. B. Park, Y. K. Sun, B. Scrosati, *Nat. Chem.* **2012**, *4*, 579–585.
- [78] L. A. Huff, H. Tavassol, J. L. Esbenshade, W. Xing, Y. M. Chiang, A. A. Gewirth, *ACS Appl. Mater. Interfaces* **2016**, *8*, 371–380.
- [79] A. Komimoto, E. Yasukawa, N. Sato, T. Ijuuin, H. Asahina, S. Mori, *J. Power Sources* **1997**, *68*, 471–475.
- [80] H. Ota, Y. Sakata, X. Wang, J. Sasahara, E. Yasukawa, *J. Electrochem. Soc.* **2004**, *151*, A437.
- [81] Q. Peng, J. Chen, H. Ji, A. Morita, S. Ye, *J. Am. Chem. Soc.* **2018**, *140*, 15568–15571.
- [82] a) Y. Matsuda, M. Ishikawa, S. Yoshitake, M. Morita, *J. Power Sources* **1995**, *54*, 301–305; b) M. Ishikawa, M. Morita, Y. Matsuda, *J. Power Sources* **1997**, *68*, 501–505.
- [83] G. M. Stone, S. A. Mullin, A. A. Teran, D. T. Hallinan, A. M. Minor, A. Hexemer, N. P. Balsara, *J. Electrochem. Soc.* **2012**, *159*, A222–A227.
- [84] M. M. Ottakam Thotiyil, S. A. Freunberger, Z. Peng, Y. Chen, Z. Liu, P. G. Bruce, *Nat. Mater.* **2013**, *12*, 1050–1056.
- [85] Z. Zhu, A. Kushima, Z. Yin, L. Qi, K. Amine, J. Lu, J. Li, *Nat. Energy* **2016**, *1*(8), 16111.
- [86] L. Qin, D. Zhai, W. Lv, W. Yang, J. Huang, S. Yao, J. Cui, W.-G. Chong, J.-Q. Huang, F. Kang, J.-K. Kim, Q.-H. Yang, *Nano Energy* **2017**, *40*, 258–263.
- [87] J. Hassoun, H. G. Jung, D. J. Lee, J. B. Park, K. Amine, Y. K. Sun, B. Scrosati, *Nano Lett.* **2012**, *12*, 5775–5779.
- [88] S. Wu, K. Zhu, J. Tang, K. Liao, S. Bai, J. Yi, Y. Yamauchi, M. Ishida, H. Zhou, *Energy Environ. Sci.* **2016**, *9*, 3262–3271.
- [89] G. A. Elia, D. Bresser, J. Reiter, P. Oberhumer, Y. K. Sun, B. Scrosati, S. Passerini, J. Hassoun, *ACS Appl. Mater. Interfaces* **2015**, *7*, 22638–22643.
- [90] A. Wang, S. Tang, D. Kong, S. Liu, K. Chiou, L. Zhi, J. Huang, Y. Y. Xia, J. Luo, *Adv. Mater.* **2018**, *30*, Article number.
- [91] L. Ye, M. Liao, H. Sun, Y. Yang, C. Tang, Y. Zhao, L. Wang, Y. Xu, L. Zhang, B. Wang, F. Xu, X. Sun, Y. Zhang, H. Dai, P. G. Bruce, H. Peng, *Angew. Chem. Int. Ed.* **2019**, *58*, 2437–2442.
- [92] K. Liao, S. Wu, X. Mu, Q. Lu, M. Han, P. He, Z. Shao, H. Zhou, *Adv. Mater.* **2018**, *30*, 1705711.
- [93] M. Asadi, B. Sayahpour, P. Abbasi, A. T. Ngo, K. Karis, J. R. Jokisaari, C. Liu, B. Narayanan, M. Gerard, P. Yasaee, X. Hu, A. Mukherjee, K. C. Lau, R. S. Assary, F. Khalili-Araghi, R. F. Klie, L. A. Curtiss, A. Salehi-Khojin, *Nature* **2018**, *555*, 502–506.
- [94] W.-J. Kwak, S.-J. Park, H.-G. Jung, Y.-K. Sun, *Adv. Energy Mater.* **2018**, *8*, 1702258.
- [95] J. J. Xu, Q. C. Liu, Y. Yu, J. Wang, J. M. Yan, X. B. Zhang, *Adv. Mater.* **2017**, *29*, 1606552.
- [96] O. Crowther, M. Salomon, *Membranes (Basel)* **2012**, *2*, 216–227.
- [97] G. A. Elia, J. Hassoun, *Solid State Ionics* **2016**, *287*, 22–27.
- [98] H. Nemori, X. Shang, H. Minami, S. Mitsuoka, M. Nomura, H. Sonoki, Y. Morita, D. Mori, Y. Takeda, O. Yamamoto, N. Imanishi, *Solid State Ionics* **2018**, *317*, 136–141.
- [99] T. Zhang, N. Imanishi, Y. Shimonishi, A. Hirano, Y. Takeda, O. Yamamoto, N. Sammes, *Chem. Commun.* **2010**, *46*, 1661–1663.
- [100] W. Choi, M. Kim, J. O. Park, J. H. Kim, K. Choi, Y. S. Kim, T. Y. Kim, K. Ogata, D. Im, S. G. Doo, Y. Hwang, *Sci. Rep.* **2017**, *7*, 12037.
- [101] B. G. Kim, J.-S. Kim, J. Min, Y.-H. Lee, J. H. Choi, M. C. Jang, S. A. Freunberger, J. W. Choi, *Adv. Funct. Mater.* **2016**, *26*, 1747–1756.
- [102] Y. B. Yin, X. Y. Yang, Z. W. Chang, Y. H. Zhu, T. Liu, J. M. Yan, Q. Jiang, *Adv. Mater.* **2018**, *30*, 1703791.
- [103] L. Wang, J. Pan, Y. Zhang, X. Cheng, L. Liu, H. Peng, *Adv. Mater.* **2017**, *29*, 1704378.
- [104] J. Zhang, W. Xu, W. Liu, *J. Power Sources* **2010**, *195*, 7438–7444.
- [105] X. B. Zhu, T. S. Zhao, Z. H. Wei, P. Tan, L. An, *Energy Environ. Sci.* **2015**, *8*, 3745–3754.

Manuscript received: February 25, 2019

Revised manuscript received: April 8, 2019

Version of record online: May 27, 2019